Drosophila melanogaster. The protein encoded by *wapl* controls heterochromatin organization and was identified as a modifier of both PEV and chromosome inheritance [2,3]. Thus, hWAPL is also expected to be involved in heterochromatin maintenance and epigenetic control.

Polycyclic aromatic hydrocarbons (PAHs) are carcinogenic and immunotoxic chemicals widely distributed in the environment [4]. 3-Methylcholanthrene (3-MC) is one of the most toxic and the best-studied compounds in the PAHs. Most of the toxic effects of PAHs are mediated by the aryl hydrocarbon receptor (AhR) [5]. When PAHs bind to the AhR, the ligated AhR translocates from the cytoplasm to the nucleus where it switches its partner molecule from heat shock protein 90 kD (Hsp90) to the aryl hydrocarbon receptor nuclear translocator (Arnt) [6]. The resulting AhR/Arnt heterodimer binds a specific DNA sequence, designated xenobiotic responsive element (XRE), in the promoter region of target genes to enhance their expression [6]. On the other hand, several studies have suggested the existence of AhR independent pathways for PAH toxicity [7,8]. In all cases, many of the putative target genes responsible for the toxicity symptoms have yet to be identified.

In the present study, we demonstrate that *hWAPL* is a target gene of 3-methylcholanthrene. The results suggest that carcinogenesis by 3-MC may involve alterations of *hWAPL* gene expression.

2. Materials and methods

2.1. Chemicals

3-Methylcholanthrene (Sigma-Aldrich Japan, Tokyo, Japan) was prepared in dimethylsulfoxide (DMSO) for cultured cells and in olive oil for treatment of mice. Aphidicolin (Wako Pure Chemical Industries, Ltd, Osaka, Japan), Nocodazole (Sigma Chemical Co., St Louis, MO) and α-naphthoflavone (Sigma) were prepared in DMSO.

2.2. Cell cultures

The human uterine cervical carcinoma-derived cell lines, SiHa, CaSki and HeLa cells, were obtained from American Type Culture Collection (ATCC), and grown in DMEM (Sigma) supplemented with 10% fetal bovine serum (FBS) (Trace Scientific Ltd, Melbourne, Australia) at 37 °C in a 5% CO_2 environment. Where indicated, SiHa cells were grown in DMEM supplemented with 10% charcoal/dextran treated FBS (CTF) (Biosource, Rockville, MD) or 0.4% (w/v) bovine serum albumin (BSA) (Trace) instead of FBS.

2.3. Immunoblot analysis

Protein samples were prepared as previously described [9]. Immunoblot analysis was performed as previously described [1].

2.4. Flow cytometric analysis

To determine cell cycle profiles, cells at different time points were harvested, washed, and fixed with a solution containing 70% ethanol and 30% PBS. After incubation overnight at 4 °C, cells were suspended in staining buffer (propidium iodide, 50 μg/ml; RNaseA, 0.1%; glucose, 1 mg/ml in PBS). Then, after incubation for 30 min at room temperature, the cells were analyzed with a FACS Vantage flow cytometer using the Cell Quest acquisition and analysis program (BD Biosciences, San Jose, CA).

2.5. Animals and treatment

C57/BL6 female mice (6 weeks old) were purchased from Oriental Yeast Co., Ltd (Tokyo, Japan). The mice received a single intraperitoneal injection of 1 ml of olive oil containing 3-MC at a dose of 80 mg/kg of body mass. The control mice were injected with olive oil alone. Uterus samples were harvested 24 and 48 h after injection and subjected to real time PCR analysis.

2.6. RNA isolation and quantitative real time PCR

First strand cDNA synthesis was performed as described [10] using M-MLV Reverse transcriptase (Invitrogen Japan, Tokyo, Japan) with Oligo $(dT)_{17}$ (for Figs. 1–3 and 6) or Random Primers (Invitrogen) (for Figs. 4 and 5).

Real time PCR analysis for *hWAPL* and human β-*actin* mRNAs was performed as described [1]

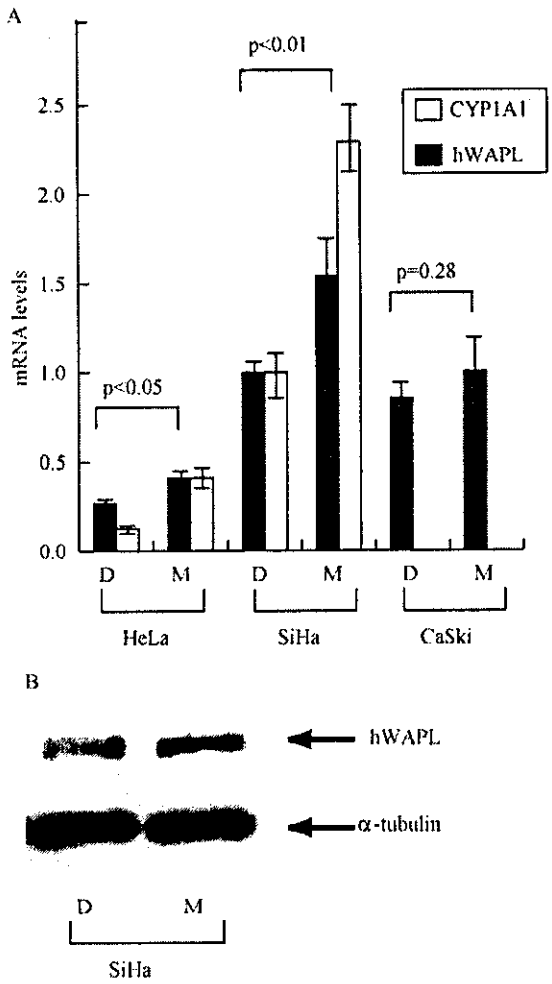

Fig. 1. Effects of 3-MC on *hWAPL* expression in the human cervical cancer-derived cell lines. D, DMSO alone; M, 3-MC. (A) HeLa, SiHa and CaSki cells were treated with 0.1% DMSO alone or 1 μM of 3-MC for 6 h. Then, the *hWAPL* and *CYP1A1* mRNA levels in the cells were evaluated by quantitative real time PCR analysis. Data were normalized to the mRNA levels of SiHa cells treated with DMSO alone that was arbitrarily set to 1 in the graphical presentation. *Bars, s.e.* (B) SiHa cells were treated with 0.1% DMSO alone or 1 μM 3MC for 6 h, and then the protein samples were prepared and subjected to western blotting analysis. α-tubulin was also shown as a loading control.

except for the 40 PCR cycles at 95 °C for 3 s and 68 °C for 30 s. Real Time PCR analysis for human *CYP1A1* mRNA and *hWAPL* hnRNA was also performed with the same PCR protocol. The nucleotide sequences of primers specific for human *CYP1A1* mRNA were previously described [11]. Primers specific for *hWAPL* hnRNA are 5′-GAGATTACACCACTGCACTCC-3′ and 5′-TTGCTCCCACTTACTATGGCC-3′. For mouse cDNAs, we used primers specific for the mouse homolog of *hWAPL* mRNA, 5′-ACCTGGTGGAGTATAGTGCCC-3′ and 5′-TGGCAGAGACACCCAAGAAGC-3′ (The nucleotide sequences were obtained from mKIAA0261 in Database), mouse β-*actin* mRNA, 5′-AGCCTTCCTTCTTGGGTATGG-3′ and 5′-CACTTGCGGTGCACGATGGAG-3′, and mouse *CYP1A1* mRNA, 5′-TTTGGTTTGGGCAAGCGA-3′ and 5′-GTCTAAGCCTGAAGATGC-3′. Reaction mixtures were denatured at 95 °C for 30 s then subjected to 40 PCR cycles at 95 °C for 3 s, 68 °C for 30 s, and 86 °C for 6 s for mouse *WAPL* mRNA, and at 95 °C for 3 s, 68 °C for 30 s, and 85 °C for 6 s for mouse β-*actin* and *CYP1A1* mRNAs, respectively. *hWAPL, mouse WAPL* and human and mouse *CYP1A1* mRNA levels and *hWAPL* hnRNA level were normalized to human and mouse β-*actin* signals, respectively. The absence of PCR products after the PCR on non-reverse-transcribed total RNA served as a routine check for contaminating genomic DNA. We performed the experiments to determine mRNA and hnRNA levels in triplicate.

The data were analyzed using Student's-*t* test, and $Ps < 0.05$ were considered to indicate significant differences.

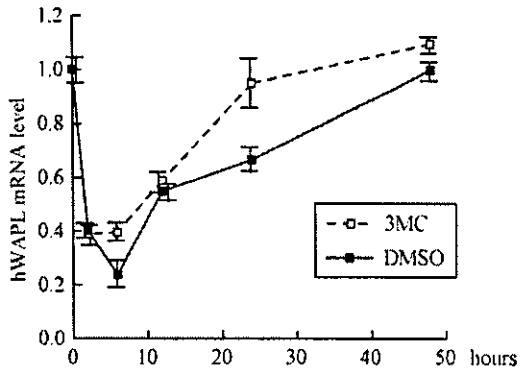

Fig. 2. Kinetics of *hWAPL* mRNA levels in SiHa cells at several time points after treatment with DMSO alone or 1 μM of 3-MC. The *hWAPL* mRNA levels in the cells were evaluated by quantitative real time PCR analysis. Data were normalized to the mRNA level at 0 h that was arbitrarily set to 1 in the graphical presentation. *Bars, s.e.*

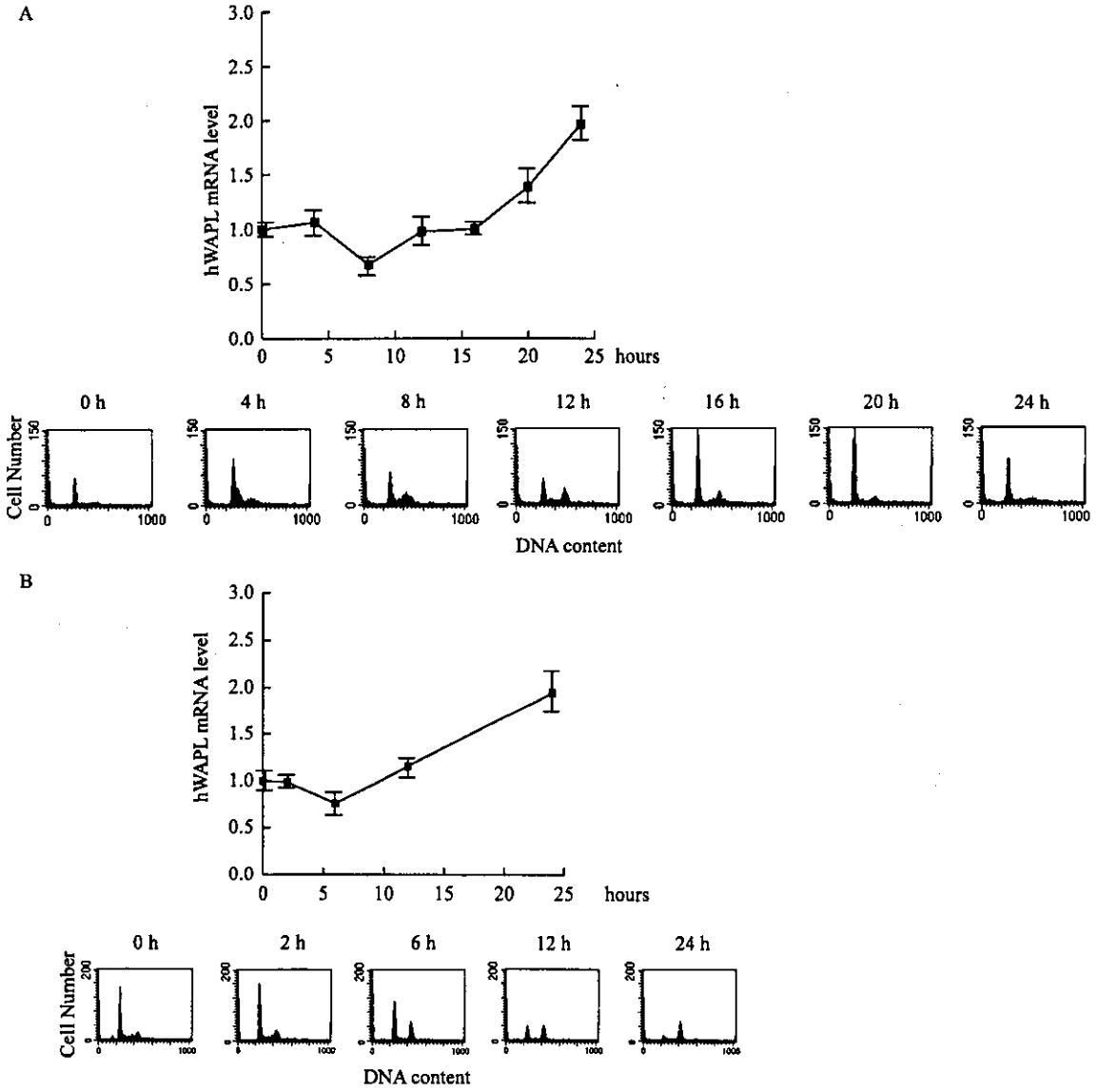

Fig. 3. Cell cycle profiles and *hWAPL* mRNA levels. *hWAPL* mRNA levels in the cells were determined by real time PCR analysis. Data were normalized to the mRNA level at 0 h that was arbitrarily set to 1 in the graphical presentation. *Bars, s.e.*. Cell cycle profiles of the cells at each time points were also confirmed by flow cytometric analysis. (A) Kinetics of *hWAPL* mRNA levels in SiHa cells at 0, 4, 8, 12, 16, 20 and 24 h after releasing from G1 arrest by 1 μg/ml aphidicolin treatment. (B) Kinetics of *hWAPL* mRNA levels in SiHa cells at 0, 2, 6, 12 and 24 h after 50 ng/ml nocodazole treatment.

3. Results and discussion

To examine whether 3-MC affects *hWAPL* expression, we treated various human uterine cervical cancer-derived cell lines with dimethylsulfoxide (DMSO) alone or 3-MC for 6 h. Then, we calculated the amounts of the *hWAPL* mRNAs in the cells by quantitative real time PCR analysis, and found that *hWAPL* mRNA levels were increased in the 3-MC-treated cells (Fig. 1A). The increases in *hWAPL* mRNA levels in SiHa cells was most remarkable among the cell lines examined. Because the *CYP1A1* gene is

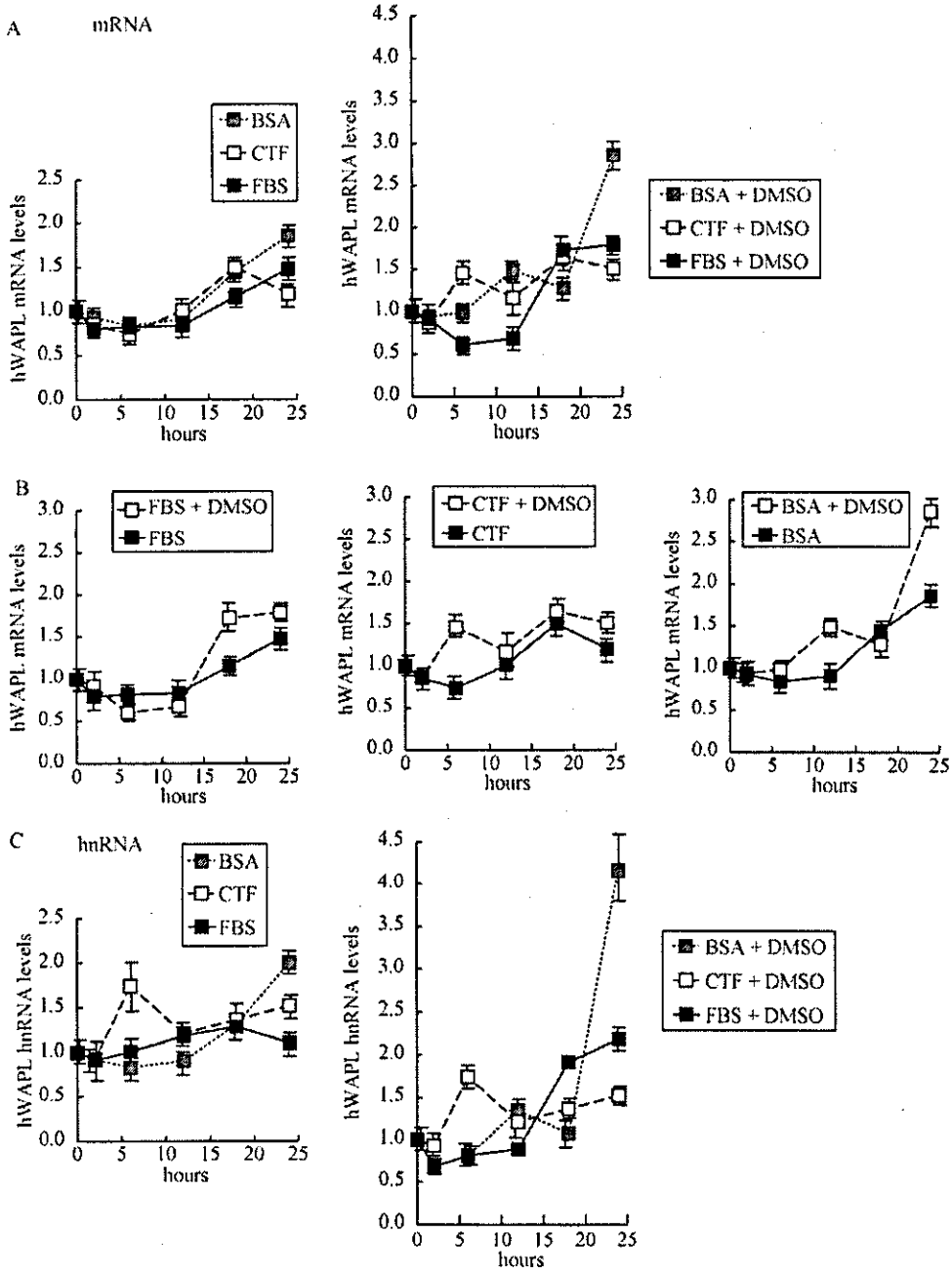

Fig. 4. Effects of FBS, CTF, BSA and DMSO on *hWAPL* mRNA and hnRNA levels in SiHa cells. *hWAPL* mRNA and hnRNA levels in SiHa cells at 0, 2, 6, 12, 18 and 24 h after replacing the growth medium to a fresh medium supplemented with FBS, CTF or BSA with or without 0.1% DMSO were deteremined by real time PCR analysis. Data were normalized to the mRNA and hnRNA level at 0 h that was arbitrarily set to 1 in the graphical presentation. *Bars, s.e.* (A) Kinetics of the *hWAPL* mRNA levels in the cells grown in the growth medium supplemented as indicated. (B) Graphical representation of the effects of DMSO on the kinetics of *hWAPL* mRNA levels in the cells grown in the growth medium supplemented with FBS, CTF or BSA. (C) Kinetics of the *hWAPL* hnRNA levels in the cells grown in the growth medium supplemented as indicated.

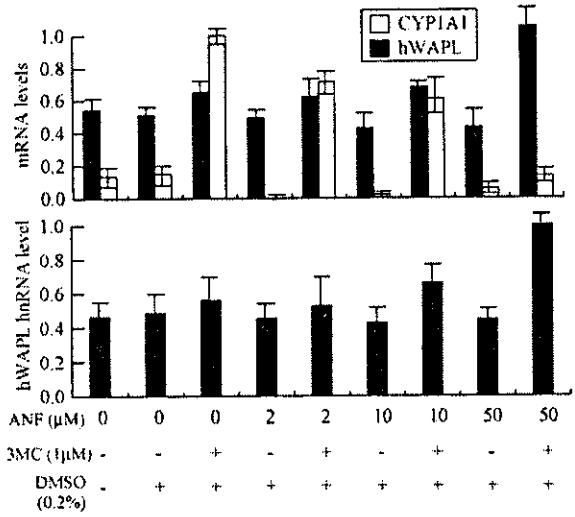

Fig. 5. Effects of AhR inhibition by α-naphthoflavone on *hWAPL* mRNA and hnRNA levels in SiHa cells treated with 3-MC. SiHa cells were treated with 0.2% DMSO alone or 1 μM 3-MC with 0. 2, 10 or 50 μM ANF for 6 h. Then, the *hWAPL* mRNA and hnRNA levels and the *CYP1A1* mRNA levels were deteremined by real time PCR analysis. SiHa cells grown for 6 h in a normal fresh medium without chemicals were also analyzed as a normal control. Data were normalized to the maximaum mRNA and hnRNA levels that were arbitrarily set to 1 in the graphical presentation. *Bars, s.e.*

a well-known target of 3-MC [12,13], we also calculated *CYP1A1* mRNA levels in the three cell lines to confirm the effects of 3-MC on the cells (Fig. 1A). We found that *CYP1A1* mRNA levels in SiHa cells were highest and increased most remarkable. *CYP1A1* mRNA in CaSki cells was not detected in our experiments. We also observed that hWAPL protein level was increased in the 3-MC-treated SiHa cells (Fig. 1B).

We next examined the effects of 3-MC on *hWAPL* expression in SiHa cells at several time points after 3-MC treatment (Fig. 2). The 3-MC-treated cells showed higher levels of *hWAPL* mRNA than the control cells at all time points examined. Interestingly, the *hWAPL* mRNA levels decreased first 6 h and then increased after changing the medium to a fresh medium containing DMSO with or without 3-MC as seen in Fig. 2.

These results prompted us to investigate whether the *hWAPL* expression is related to the cell cycle. First, to synchronize cell cycle progression, we treated SiHa cells with aphidicolin, an inhibitor of DNA synthesis, for 12 h to induce G1-phase arrest. We then released the cells from G1 arrest by changing the culture medium to a fresh growth medium. The synchronized cells were harvested every 4 h for 24 h after release from aphidicolin, and the *hWAPL* mRNA levels were calculated by quantitative real time PCR analysis (Fig. 3A). As seen in Fig. 3A, *hWAPL* mRNA initially decreased and then increased over time. Flow cytometric analysis confirmed the cell cycle phase of the cells at each time point (Fig. 3A). From these results, *hWAPL* mRNA level seemed to fluctuate in accordance with cell cycle profile. However, the levels of *hWAPL* mRNA in the cells treated with nocodazole, an inhibitor of spindle assembly, fluctuated in a similar manner to the aphidicolin-synchronized cells (Fig. 3B). Thus, amounts of *hWAPL* mRNAs are likely to have no relation to the cell cycle profiles. Recently, Guigal et al. demonstrated that FBS induces transcription of the *CYP1A1* gene. Therefore, we suspected that the fluctuation of *hWAPL* mRNA levels might be associated with the culture medium change.

To investigate the effects of components in FBS on the fluctuation of *hWAPL* mRNA levels, we examined the *hWAPL* mRNA levels in SiHa cells after changing growth medium to a fresh medium supplemented with charcoal/dextran treated FBS (CTF) or BSA instead of FBS. The fluctuations of the *hWAPL* mRNA levels showed similar trends among the cells grown with FBS, CTF and BSA (Fig. 4A; left panel). However, all cells examined in Figs. 1–3 were grown in the medium containing DMSO. Thus, we also tested the effects of DMSO with FBS, CTF or BSA at the same time. Interestingly, fluctuations of the *hWAPL* mRNA levels in SiHa cells treated with 0.1% DMSO showed different trends among FBS, CTF and BSA (Fig. 4A; right panel), and the *hWAPL* mRNA levels in the DMSO-treated cells fluctuated more drastically than that in the cells grown without DMSO (Fig. 4B). Especially, remarkable decrease of *hWAPL* mRNA levels for first 6 h after the medium change was distinctive for the growth medium supplemented with FBS and DMSO. These results suggest that DMSO and some constituents of FBS affect *hWAPL* mRNA accumulation synergistically.

mRNA levels do not always reflect on the transcription activity of genes. To investigate the kinetics of the promoter activities of the *hWAPL* gene in the cells, we evaluated the levels of *hWAPL* heterogeneous nuclear RNA (hnRNA), the unprocessed precursor of the mature and functional mRNA,

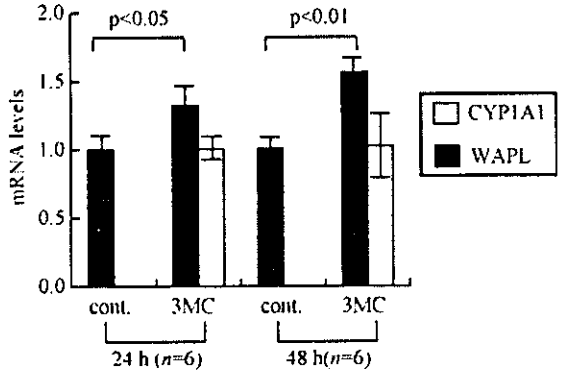

Fig. 6. Effects of 3-MC on *WAPL* mRNA levels in mouse uteri. The mice received a single intraperitoneal injection of 1 ml of olive oil containing 3-MC (3-MC) or olive oil only (cont.), and *WAPL* mRNA levels in the uteri at 24 and 48 h after injection were determined with quantitative real time PCR analysis. *CYP1A1* mRNA levels were also deteremined to confirm the effects of 3-MC on mouse uteri. The data represent the means of multiple samples normalized to the mean values of the *hWAPL* mRNA levels in the cont. 24 h samples and *CYP1A1* mRNA levels in the 3-MC 24 h samples, respectively, that were arbitrarily set to 1 in the graphical presentation. *Bars, s.e.*

by real time PCR using intron-specific primers for *hWAPL* searched in Ensembl Genome Browser (http://www.ensembl.org/). Levels of hnRNA have been proposed as a surrogate for nuclear run-on assays to determine gene transcription rates [14,15]. Although the *hWAPL* hnRNA levels fluctuated in somewhat different manner to the mRNA levels in the cells grown without DMSO, the *hWAPL* hnRNA levels in the DMSO-treated cells fluctuated in similar manner to the mRNA levels (Fig. 4C; compare with Fig. 4A). These results suggest that DMSO and some components of FBS affect transcriptional activity of the *hWAPL* gene. Increase of *hWAPL* transcription levels at 24 h in common with the cells under various conditions may be caused by the accumulation of wastes in their growth medium.

3-MC is known to be an agonist of AhR [16]. Thus, to investigate whether AhR is related to *hWAPL* transcription activation, we examined the effects of α-naphthoflavone (ANF), an AhR antagonist [17], at a dose of 2, 10 and 50 μM on *hWAPL* mRNA and hnRNA levels in 3-MC-treated SiHa cells by quantitative real time PCR analysis (Fig. 5). We also evaluated *CYP1A1* mRNA levels for monitoring the inhibitory effects on AhR functions by ANF, and found that 50 μM of ANF strongly inhibited AhR functions (Fig. 5; upper panel). Interestingly, increase of *hWAPL* mRNA levels by 3-MC was more remarkable in AhR-inhibited cells rather than that in AhR-functioning normal cells. Induction of *hWAPL* hnRNA levels showed similar manner to the *hWAPL* mRNA (Fig. 5; lower panel). From these results, we hypothesized that AhR was involved in the transcriptional regulation of *hWAPL*, but there are complex mechanisms for the transcriptional regulation of *hWAPL*. We did not find XRE motif in 5000 bp of 5′-upstream sequence of the *hWAPL* gene using MOTIF Sequence Motif Search (http://motif.genome.jp/) at the cut off score 85. Thus, although further investigation is required, we suppose that *hWAPL* is not a direct target of 3-MC but a down stream molecule of a 3-MC-targeted molecule.

Finally, we examined whether the mRNA level of a mouse homolog of *hWAPL* is increased by 3-MC in mouse uterus. Twenty-four and 48 h after the injection of 3-MC into the abdominal cavities of C57/BL6 female mice, we harvested the uteri and analyzed the *WAPL* mRNA levels by quantitative real time PCR analysis. The *CYP1A1* mRNA levels were also analyzed to confirm the 3-MC effects on the uteri. The uteri exhibited increases in *WAPL* mRNA levels compared with that of control mice (Fig. 6). These data suggest that 3-MC exposure affects *WAPL* expression in uterus.

Our recent data demonstrated that the unscheduled increase of *hWAPL* expression in human uterine cervix is associated with cervical cancer [1]. In Addition, previous studies demonstrated that 3-MC induces carcinogenesis in mouse uterine cervix [18, 19]. Thus, although the *hWAPL* induction by 3-MC was weak in our experiments, our results suggest that the promotion of carcinogenesis by 3-MC in uterus is likely to involve the *hWAPL* oncogene.

Acknowledgements

This work was supported by a Grant-in-Aid for scientific research on Priority Area (C) from the Ministry of Education, Science, Sports and Culture, and a grant from Core Research for Evolutional Science and Technology (CREST), Japan Science and Technology Corporation.

References

[1] K. Oikawa, T. Ohbayashi, T. Kiyono, H. Nishi, K. Isaka, A. Umezawa, et al., Expression of a novel human gene, human wings apart-like (hWAPL), is associated with cervical carcinogenesis and tumor progression, Cancer Res. 64 (2004) 3545–3549.

[2] F. Verni, R. Gandhi, M.L. Goldberg, M. Gatti, Genetic and molecular analysis of wings apart-like (wapl), a gene controlling heterochromatin organization in *Drosophila melanogaster*, Genetics 154 (2000) 1693–1710.

[3] K.W. Dobie, C.D. Kennedy, V.M. Velasco, T.L. McGrath, J. Weko, R.W. Patterson, G.H. Karpen, Identification of chromosome inheritance modifiers in *Drosophila melanogaster*, Genetics 157 (2001) 1623–1637.

[4] S. Reynaud, C. Duchiron, P. Deschaux, 3-Methylcholanthrene increases phorbol 12-myristate 13-acetate-induced respiratory burst activity and intracellular calcium levels in common carp (Cyprinus carpio L) macrophages, Toxicol. Appl. Pharmacol. 175 (2001) 1–9.

[5] J. Mimura, Y. Fujii-Kuriyama, Functional role of AhR in the expression of toxic effects by TCDD, Biochim. Biophys. Acta 1619 (2003) 263–268.

[6] K. Sogawa, Y. Fujii-Kuriyama, Ah receptor, a novel ligand-activated transcription factor, J. Biochem. (Tokyo) 122 (1997) 1075–1079.

[7] K. Oikawa, T. Ohbayashi, J. Mimura, R. Iwata, A. Kameta, K. Evine, et al., Dioxin suppresses the checkpoint protein, MAD2, by an aryl hydrocarbon receptor-independent pathway, Cancer Res. 61 (2001) 5707–5709.

[8] S.R. Kondraganti, P. Fernandez-Saluguero, F.J. Gonzalez, K.S. Ramos, W. Jiang, B. Moorthy, Polycyclic aromatic hydrocarbon-inducible DNA adducts: evidence by 32P-postlabeling and use of knockout mice for Ah receptor-independent mechanisms of metabolic activation in vivo, Int. J. Cancer 103 (2003) 5–11.

[9] K. Oikawa, T. Ohbayashi, J. Mimura, Y. Fujii-Kuriyama, S. Teshima, K. Rokutan, et al., Dioxin stimulates synthesis and secretion of IgE-dependent histamine-releasing factor, Biochem. Biophys. Res. Commun. 290 (2002) 984–987.

[10] M. Kuroda, T. Ishida, M. Takanashi, M. Satoh, R. Machinami, T. Watanabe, Oncogenic transformation and inhibition of adipocytic conversion of preadipocytes by TLS/FUS-CHOP type II chimeric protein, Am. J. Pathol. 151 (1997) 735–744.

[11] K. Oikawa, Y. Kosugi, T. Ohbayashi, A. Kameta, K. Isaka, M. Takayama, et al., Increased expression of IgE-dependent histamine-releasing factor in endometriotic implants, J. Pathol. 199 (2003) 318–323.

[12] N. Guigal, E. Seree, V. Bourgarel-Rey, Y. Barra, Induction of CYP1A1 by serum independent of AhR pathway, Biochem. Biophys. Res. Commun. 267 (2000) 572–576.

[13] N. Guigal, E. Seree, Q.B. Nguyen, B. Charvet, A. Desobry, Y. Barra, Serum induces a transcriptional activation of CYP1A1 gene in HepG2 independently of the AhR pathway, Life Sci. 68 (2001) 2141–2150.

[14] C.J. Elferink, J.J. Reiners Jr., Quantitative RT-PCR on CYP1A1 heterogeneous nuclear RNA: a surrogate for the in vitro transcription run-on assay, Biotechniques 20 (1996) 470–477.

[15] R.F. Johnson, C.M. Mitchell, W.B. Giles, W.A. Walters, T. Zakar, The in vivo control of prostaglandin H synthase-2 messenger ribonucleic acid expression in the human amnion at parturition, J. Clin. Endocrinol. Metab. 87 (2002) 2816–2823.

[16] M. Naruse, Y. Ishihara, S. Miyagawa-Tomita, A. Koyama, H. Hagiwara, 3-Methylcholanthrene, which binds to the arylhydrocarbon receptor, inhibits proliferation and differentiation of osteoblasts in vitro and ossification in vivo, Endocrinology 143 (2002) 3575–3581.

[17] T.A. Gasiewicz, G. Rucci, Alpha-naphthoflavone acts as an antagonist of 2,3,7, 8-tetrachlorodibenzo-p-dioxin by forming an inactive complex with the Ah receptor, Mol. Pharmacol. 40 (1991) 607–612.

[18] P. Das, A.R. Rao, P.N. Srivastava, Influence of ascorbic acid on MCA-induced carcinogenesis in the uterine cervix of mice, Cancer Lett. 72 (1993) 121–125.

[19] S. Gagandeep, S. Dhanalakshmi, E. Mendiz, A.R. Rao, R.K. Kale, Chemopreventive effects of Cuminum cyminum in chemically induced forestomach and uterine cervix tumors in murine model systems, Nutr. Cancer 47 (2003) 171–180.

Int. J. Cancer: **112**, 365–375 (2004)

Publication of the International Union Against Cancer

LOW EXPRESSION OF HUMAN TUBULIN TYROSINE LIGASE AND SUPPRESSED TUBULIN TYROSINATION/DETYROSINATION CYCLE ARE ASSOCIATED WITH IMPAIRED NEURONAL DIFFERENTIATION IN NEUROBLASTOMAS WITH POOR PROGNOSIS

Chiaki KATO[1,2], Kou MIYAZAKI[1], Atsuko NAKAGAWA[3], Miki OHIRA[1], Yohko NAKAMURA[1], Toshinori OZAKI[1], Toshio IMAI[2] and Akira NAKAGAWARA[1]*

[1]*Division of Biochemistry, Chiba Cancer Center Research Institute, Chiba, Japan*
[2]*Department of Physiologic Chemistry Faculty of Science, Toho University, Chiba, Japan*
[3]*Second Department of Pathology, Aichi Medical University, Nagakute, Japan*

Neuroblastoma (NBL), one of the most common childhood solid tumors, has a distinct nature in different prognostic subgroups. However, the precise mechanism underlying this phenomenon remains largely unknown. To understand the molecular and genetic bases of neuroblastoma, we have generated its cDNA libraries and identified a human ortholog of *tubulin tyrosine ligase* gene (*hTTL/Nbla0660*) as a differentially expressed gene at high levels in a favorable subset of the tumor. Tubulin is subjected to several types of evolutionarily conserved posttranslational modification, including tyrosination and detyrosination. Tubulin tyrosine ligase catalyzes ligation of the tyrosine residue to the COOH terminus of the detyrosinated form of α-tubulin. The measurement of *hTTL* mRNA expression in 74 primary neuroblastomas by quantitative real-time reverse transcription-PCR revealed that its high expression was significantly associated with favorable stages (1, 2 and 4s; $p = 0.0069$), high *TrkA* expression ($p = 0.002$), a single copy of *MYCN* ($p < 0.00005$), tumors found by mass screening ($p = 0.0042$), nonadrenal origin ($p = 0.0042$) and good prognosis ($p = 0.023$). The log-rank test showed that high expression of *hTTL* was an indicator of favorable prognosis ($p = 0.026$). Immunohistochemical analysis using specific antibodies generated by us demonstrated that tyrosinated tubulin (Tyr-tubulin), detyrosinated tubulin (Glu-tubulin) and hTTL as well as Δ2-tubulin were positive in favorable tumors, whereas only Δ2-tubulin was positive in the tumors with *MYCN* amplification. In an RTBM1 neuroblastoma cell line, hTTL was increased after treating the cells with bone morphogenetic protein 2 (BMP2) or all-trans retinoic acid (RA), which induced neuronal differentiation. These results suggest that the deregulated tubulin tyrosination/detyrosination cycle caused by decreased expression of hTTL is associated with inhibition of neuronal differentiation and enhancement of cell growth in the primary neuroblastomas with poor outcome.

Key words: *tubulin tyrosine ligase; tubulin tyrosination; neuroblastoma; neuronal differentiation; prognostic factor*

Tubulin is one of the most important molecular components that regulate cytoskeletal structure relating to cell motility, cell division, differentiation, invasion and metastasis in cancer. However, functional modification of tubulin protein has still been elusive. Tubulin is subjected to several types of evolutionarily conserved posttranslational modification that includes tyrosination/detyrosination, acetylation, phosophorylation, palmitoylation, polyglutamylation and polyglycylation.[1–4] The discovery of tyrosination cycle stems from the serial observations that the addition of radiolabeled tyrosine to a rat brain cytosolic extract leads to tyrosination of the COOH terminus of a single endogenous protein, α-tubulin, by a translation-independent mechanism.[5–7] Posttranslational incorporation of tyrosine into the tubulin has also been shown to occur *in vivo*.[8–10] The cycle of tyrosination/detyrosination is evolutionarily conserved[11–13] and is regulated by both tubulin tyrosine ligase (TTL) and carboxypeptidase, the gene of which has not yet been identified (Fig. 1). Microtubule dynamics is also an important factor. TTL protein was first purified by immunoaffinity chromatography from the lysates of bovine and porcine brains and was extensively characterized by protein sequencing.[14] Recently, rat *TTL* cDNA has also been isolated.[15] Interestingly, in 1991, Paturle-Lafanechere *et al.*[16] identified a nontyrosinatable variant of tubulin that lacked 2 amino acid residues, glutamic acid and tyrosine, at the COOH terminus (Δ2-tubulin). Δ2-tubulin was found to accumulate in mature neurons and in stable microtubule assemblies in cells.[17,18] In some tumors, it also accumulated in the cellular cytoplasm in association with decreased levels of TTL, suggesting that the amount of Δ2-tubulin and TTL expression level in tumor cells are important to define the malignant grade of cancer.[19] However, pathophysiologic significance of the tyrosination/detyrosination cycle in normal and cancer cells still remains unclear.

Neuroblastoma (NBL) is one of the most common childhood solid tumors and has distinct biologic characteristics in different prognostic subgroups. For example, NBL in patients under 1 year of age usually regresses spontaneously, whereas that in patients over 1 year of age often grows aggressively and eventually kills the patient. To understand the molecular mechanism of distinct biology and tumorigenesis of NBL, we have previously performed a comprehensive approach to unveil the gene expression profiles among the NBL subsets.[20,21] We constructed the subset-specific oligo-capping cDNA libraries from the primary NBL tissues with favorable (stage 1, high expression of *TrkA* and a single copy of *MYCN*) and unfavorable (stage 3 or 4, decreased expression of *TrkA* and *MYCN* amplification) characteristics and randomly cloned 4,654 cDNAs. After adding the cDNAs obtained from the stage 4s NBL cDNA library to our NBL gene collection, we made an in-house cDNA microarray carrying 5,340 genes proper to NBL. The comprehensive analysis of 136 NBLs using the microar-

Abbreviations: BMP2, bone morphogenetic protein 2; DMEM, Dulbecco's modified Eagle's medium; ECL, enhanced chemiluminescence; FBS, fetal bovine serum; hTTL, human tubulin tyrosine ligase; NBL, neuroblastoma; RA, retinoic acid; TCP, tubulin carboxypeptidase; TTL, tubulin tyrosine ligase.

Grant sponsor: Grant-in-Aid for Scientific Research and for Scientific Research on Priority Areas, Medical Genome Science from the Ministry of Education, Science, Sports and Culture, Japan; Grant sponsor: Hisamitsu Pharmaceutical Co. Inc.

*Correspondence to: Division of Biochemistry, Chiba Cancer Center Research Institute, 666-2 Nitona, Chuoh-ku, Chiba 260-8717, Japan. Fax: +81-43-265-4459. E-mail: akiranak@chiba-ccri.chuo.chiba.jp

Received 27 January 2004; Accepted 15 April 2004

DOI 10.1002/ijc.20431
Published online 23 June 2004 in Wiley InterScience (www.interscience.wiley.com).

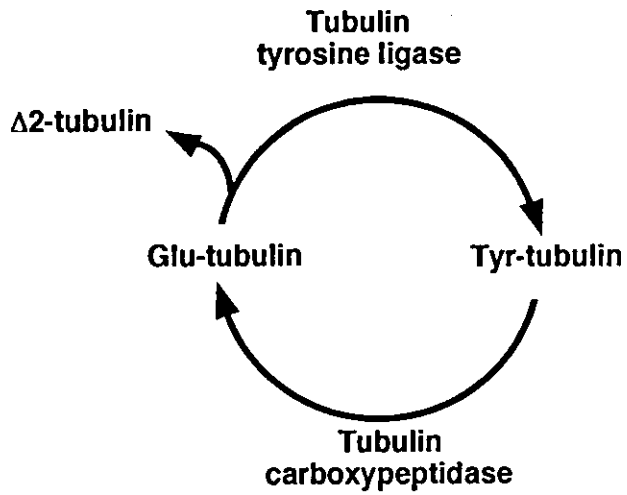

FIGURE 1 – The tyrosination/detyrosination cycle catalyzed by tubulin tyrosine ligase and tubulin carboxypeptidase.

ray showed that many genes that are related to the cytoskeletal components, including α-tubulin, had prognostic significance (data not shown).

In the present study, we have cloned for the first time the human ortholog of TTL (*hTTL*) from both the NBL and a fetal brain cDNA libraries. The analysis using 74 primary NBLs shows that expression of *hTTL* mRNA is significantly lower in unfavorable NBLs than in favorable tumors. The examination using specific antibodies raised against hTTL, Tyr-tubulin, Glu-tubulin and Δ2-tubulin demonstrates that hTTL is increased during induction of neuronal differentiation of cultured NBL cells treated with BMP2 or RA. The immunohistochemical study shows that hTTL, Tyr-tubulin, Glu-tubulin and Δ2-tubulin are positive in favorable NBLs, whereas only Δ2-tubulin is positive in aggressive NBLs with *MYCN* amplification. These suggested that the tyrosination/detyrosination cycle of α-tubulin is active in NBLs with high potential to differentiate or undergo apoptosis, while it is disregulated by downregulation of hTTL in *MYCN*-amplified NBLs, resulting in accumulation of Δ2-tubulin.

MATERIAL AND METHODS

Tumor specimen

Fresh frozen tumor tissues obtained by surgery or biopsy were sent to the Division of Biochemistry, Chiba Cancer Center Research Institute, from various hospitals in Japan with informed consent. Ninety tumors examined in this study were staged according to the International Neuroblastoma Staging System (INSS).[22] The number of tumors subjected to quantitative real-time RT-PCR were 24 in stage 1, 11 in stage 2, 5 in stage 4s, 10 in stage 3 and 24 in stage 4. The patients were treated according to the protocols previously described.[23] Biologic information on each tumor, including *MYCN* gene copy number, *TrkA* gene expression and DNA ploidy, was analyzed in our laboratory as described previously.[24]

Cell culture and transfection

COS7 and HEK293T cells were maintained in Dulbecco's modified Eagle's medium (DMEM) supplemented with 10% heat-inactivated fetal bovine serum (FBS; Life Technologies, Gaithersburg, MD) and penicillin (100 IU/ml)/streptomycin (100 μg/ml). Human neuroblastoma RTBM1 cells were grown in RPMI-1640 medium containing 10% heat-inactivated FBS and antibiotic mixture. Cultures were maintained at 37°C in a water-saturated atmosphere of 5% CO_2 in air. Transient transfection was performed by LipofectAMINE 2000 transfection reagent (Invitrogen, Carlsbad, CA) according to the manufacturer's instructions. In brief, cells were seeded in tissue culture plates to achieve 50% confluence. Twenty-four hours later, cells were transfected by using a mixture of the expression plasmids and LipofectAMINE 2000 transfection reagent in DMEM without serum. Forty-eight hours after transfection, cells were collected and analyzed by Western blotting. For neurite extension assays, RTBM1 cells were treated either with recombinant human BMP2 (Yamanouchi Pharmaceutical, Tokyo, Japan) or with RA at a final concentration of 1 nM or 5 μM, respectively.

RNA isolation and semiquantitative RT-PCR

Total RNA was prepared from neuroblastoma tissues according to the AGPC method.[25] Five micrograms of total RNA were subjected to the synthesis of the first-strand cDNA with $pd(N)_6$ random hexamer (Takara Shuzo, Otsu, Japan) and a Superscript II reverse transcriptase (Invitrogen) at 42°C for 90 min. The resultant cDNA was diluted to be a 1:20 solution and was amplified in a final volume of 10 μl of reaction mixture containing 100 μM of each deoxynucleoside triphosphate, 1 × PCR buffer, 1 μM of each primer and 0.2 U of rTaq DNA polymerase (Takara Bio, Ohtsu, Japan). The following primers were used: *hTTL*, 5′-CAGCTCTTCGGCTTTGACTT-3′ (sense) and 5′-GCTGTGGGCTGGATAAAGAG-3′ (antisense); human *GAPDH*, 5′-ACCTGACCTGCCGTCTAGAA-3′ (sense) and 5′-TCC ACCACCCTGTTGCTGTA-3′ (antisense). PCR templates were standardized by its *GAPDH* expression before performing semiquantitative PCR experiment. The PCR-amplified products were separated by electrophoresis on a 1.5% agarose gel and visualized by ethidium bromide poststaining.

Quantitative real-time RT-PCR

cDNA was prepared by the same method as in the semiquantitative RT-PCR and 2 μl of the 40-fold dilution was used for each PCR reaction. Primers and TaqMan probes for *hTTL* were designed using the primer design software Primer Express (Perkin-Elmer Applied Biosystems, Foster City, CA). The primer sequences for *hTTL* are 5′-AAGGAACTGCCTCCTGAGC-3′ and 5′-TCAATGAGCCAC ACCTTCA-3′. The probe sequence for *TTL* is 5′-FAM-ATTAGC ACCAAGCACCTCCCTTACCAGAGC-TAMRA-3′. PCR was carried out with the ABI Prism 7700 Sequence Detection System (Perkin-Elmer Applied Biosystems). Two μl of cDNA was amplified in a final volume of 25 μl containing 1 × TaqMan mixture, 300 nM each primer and 200 nM TaqMan probe. The thermal cycling condition was as follows: 50 cycles of a 2-step PCR (95°C for 15 sec, 60°C for 1 min) after the initial activation of UNG followed by denaturation (50°C for 2 min, 95°C for 10 min). TaqMan *GAPDH* control reagent kit (Roche Molecular Biochemicals, Basel, Switzerland) was used for the amplification of *GAPDH* according to the manufacturer's instructions; all data were normalized using *GAPDH* expression. The experiments were performed in triplicate for each data point.

Generation of polyclonal anti-hTTL antibodies

The polyclonal anti-hTTL antibody was raised in rabbits against Cys-coupled synthetic peptides derived from hTTL (222-RTASEPY-HVDNFQDKTCHLTNH-243 and 244-CIQKEYSKNYGKYEE-GNE-261). The polyclonal anti-Tyr-tubulin, anti-Glu-tubulin and anti-Δ2-tubulin antibodies were raised in rabbits immunized with Cys-coupled synthetic peptides corresponding to their COOH termini (CEEEGEEY, CGEEEGEE and CEGEEEGE, respectively). Antibodies were purified by using peptide-coupled affinity columns and tested for their ability to identify the corresponding proteins by Western blots. The synthetic peptides and antibodies were generated by Protein Express (Chiba, Japan).

Construction of FLAG-tagged hTTL expression plasmid

The FLAG-tagged hTTL expression plasmid was generated by PCR amplification using the cDNA library derived from human fetal brain (Stratagene, La Jolla, CA) and an *hTTL* cDNA that lacked the 5′-portion encoding the NH_2 terminal region of hTTL as templates. The forward and reverse primers used were 5′-TAAATAGTCGACGATATCATGGACTACAAGGACGAC

GACGACAAGTACACCTTCGTGGTACGCGATGAGAACAGC AGCGTCTACGCCGAGGTCTCCCGGCTGCTCCTCGCCA-3′ (sequence encoding FLAG epitope tag is in boldface, and *Eco*RV recognition site is underlined) and 5′-TACATGTCGACGCGG CCGCTCACAGCTTGAT GAA-3′ (*Not*I restriction site is underlined). The resulting PCR product was gel-purified, digested with *Eco*RV and *Not*I, inserted into identical restriction sites of a mammalian expression plasmid pIRESpuro2 (Clontech Laboratories, Palo Alto, CA) and its nucleotide sequence was verified by automated dideoxy terminator cycle sequencing.

Western blot analysis

Cells were washed in ice-cold phosphate-buffered saline (PBS), collected by centrifugation and lysed in 1 × sample buffer. Equal amounts of whole-cell lysates were fractionated by SDS-polyacrylamide gel electrophoresis (SDS-PAGE), and electrophoretically transferred onto a polyvinylidene difluoride (PVDF) membrane filter (Immobilon-P; Millipore, Billerica, MA). The filter was then blocked with Tris-buffered saline (TBS) containing 5% nonfat dry milk at room temperature for 1 hr and subsequently incubated for 1 hr with the antibodies against hTTL, Tyr-tubulin, Glu-tubulin, Δ2-tubulin, α-tubulin (5H1; PharMingen, San Diego, CA) and actin (20-33; Sigma Chemical, St. Louis, MO). The filter was further incubated with horseradish peroxidase-conjugated mouse or rabbit IgG secondary antibody (Cell Signaling Technologies, Beverly, MA). Immunoreactivity was detected using the enhanced chemiluminescence system (ECL; Amersham Pharmacia Biotechnology, Uppsala, Sweden) according to the manufacturer's instructions. The films were exposed at multiple time points to ensure that the images were not saturated.

Immunohistochemistry

Immunohistochemical stainings with antibodies against hTTL (1:100), Tyr-tubulin (1:100), Glu-tubulin (1:100) and Δ2-tubulin (1:100) were performed on 10 human neuroblastoma tumors selected from the surgical pathology file at the Department of Pathology, Aichi Medical University, based on the results of histopathology evaluation[26] and *MYCN* status. Also performed were immunostainings with antibodies against TrkA (1:40, 763; Santa Cruz Biotechnology, Santa Cruz, CA), CD56 (1B6; Novocastra Laboratories, Peterborough, U.K.) and Ki-67 (1:200, MIB-1; Dako, Kyoto, Japan) on the same tumor tissues. All of those tumor samples were obtained prior to chemotherapy and irradiation therapy and included 6 favorable histology cases with nonamplified *MYCN* (FH&NA) and 4 unfavorable histology cases with amplified *MYCN* (UH&A). Among the neuroblastoma cases, tumors in the FH&NA subset were reported to be the most favorable biologically and clinically. In contrast, tumors in the UH&A subset are known to be the most aggressive with the poorest clinical outcome.[27] Four μm thick sections from the formalin-fixed and paraffin-embedded tissue samples were deparaffinized and microwaved for 3 × 5 min in Na-citrate buffer (pH 6.0) for antigen retrieval. The slides were first immersed in 0.3% hydrogen peroxide in methanol for 20 min and then in 10% normal goat serum for 30 min. The primary antibodies were then applied at 4°C overnight, followed by a standard staining procedure using the Vectastain ABC kit (Vector Laboratories, Burlingame, CA). Sections were counterstained with hematoxylin for light microscopic review and evaluation. hTTL, Tyr-tubulin, Glu-tubulin and Δ2-tubulin were always positively detected in the cytoplasm and neuritic processes of normal ganglion cells in the separate positive control sections as well as in the test sections as built-in control, whenever available. As for the negative controls of hTTL, Tyr-tubulin, Glu-tubulin, Δ2-tubulin and TrkA stainings, normal rabbit immunoglobulins (1:500 dilution, Vector Laboratories) were applied as the primary antibody. As for the negative controls of CD56 and Ki-67 stainings, we followed the staining procedure without the primary antibodies.

Statistical analysis

Student's *t*-tests were used to explore possible associations between *hTTL* expression and other factors, such as age. Since the values of the *hTTL* expression were skewed, a log transformation was used to achieve the normality when using *t*-test and Cox regression. The distinction between high and low levels of *hTTL* was based on the median value (low, *hTTL* < 95 e.u.; high, *hTTL* > 95 e.u.), regardless of tumor stage, *MYCN* copy number, or survival. Kaplan-Meier survival curves were calculated, and survival distributions were compared using the log-rank test. Cox regression models were used to explore associations between *hTTL* expression, age, *MYCN* amplification, mass screening, origin and survival. Statistical significance was declared if the *p*-value was < 0.05. Statistical analysis was performed using Stata 7.0. (Stata, College Station, TX).

RESULTS

Cloning and expression of hTTL *gene*

We have previously constructed oligo-capping cDNA libraries from 3 fresh human NBL tissues (stages 1 and 2, high *TrkA* expression and a single copy of *MYCN*), which were gradually undergoing spontaneous regression probably due to neuronal apoptosis.[20] Screening of 1,152 novel genes by reverse transcriptase (RT)-PCR revealed that 194 genes were expressed differentially between NBLs with favorable prognosis and those with unfavorable outcome. Among them, we detected a partial cDNA sequence (*Nbla00660*) corresponding to the human ortholog of *tubulin tyrosine ligase* (*hTTL*) gene. We then cloned the full-length *hTTL* cDNA using both conventional phage library screening and genome sequence-based RT-PCR procedure. The *hTTL* gene was mapped to chromosome 2q13 and consisted of 7 exons (Fig. 2*a*) with 377 predicted amino acids (Genbank/DDBJ accession number AB071393; Fig. 2*b*). Comparison of the deduced amino acid sequence of human *TTL* cDNA with those of mouse, rat, pig and cow showed identity by 94%, 94%, 93% and 94%, respectively. *hTTL* was ubiquitously expressed in various human tissues including heart, kidney, lung, colon, thymus, spleen, mammary gland, testis, prostate, brain, cerebellum, liver, fetal brain, fetal liver, adrenal gland and skeletal muscle (Fig. 2*c*). However, it was rather preferentially expressed in adult and fetal brains and lung.

Specific antibodies and catalytic activity of hTTL

To study the role of hTTL and the tyrosination/detyrosination cycle regulated by TTL in neuroblastoma, we generated specific antibodies against human Tyr-tubulin, Glu-tubulin and Δ2-tubulin based on the previous reports.[16,18,28] The PVDF membranes spotted with equal amount (1 μg) of synthetic peptides corresponding to COOH terminal 7 amino acid residues of Tyr-tubulin (CEEEGEEY), Glu-tubulin (CGEEEGEE) and Δ2-tubulin (CEGEEEGE) were immunoblotted with rabbit anti-Tyr-tubulin antibody (Fig. 3*a*, top), anti-Glu-tubulin antibody (Fig. 3*a*, middle) and anti-Δ2-tubulin antibody (Fig. 3*a*, bottom), respectively. There were no crossreactivities among them, suggesting that those 3 antibodies were highly specific to each form of tubulin. To confirm the catalytic activity of hTTL encoded by the gene we cloned, we transfected the HEK293T cells with various amount of *hTTL* expression construct. Increased levels of hTTL in those cells induced tyrosination of tubulin in dose-dependent manner, while the level of endogenous Glu-tubulin was decreased (Fig. 3*c*). These results showed that hTTL protein encoded by the gene we cloned has its catalytic activity.

Upregulation of hTTL expression during neuronal differentiation

BMP2 has been characterized as a neurotrophic factor.[29] Recently, Nakamura *et al.*[30] have reported that RTBM1, a human neuroblastoma cell line, is responsive to both BMP2 and RA by extending neurites. By using this system, we examined whether the expression levels of hTTL change during induction of neuronal differentiation. As shown in Figure 4, the treatment of RTBM1

a

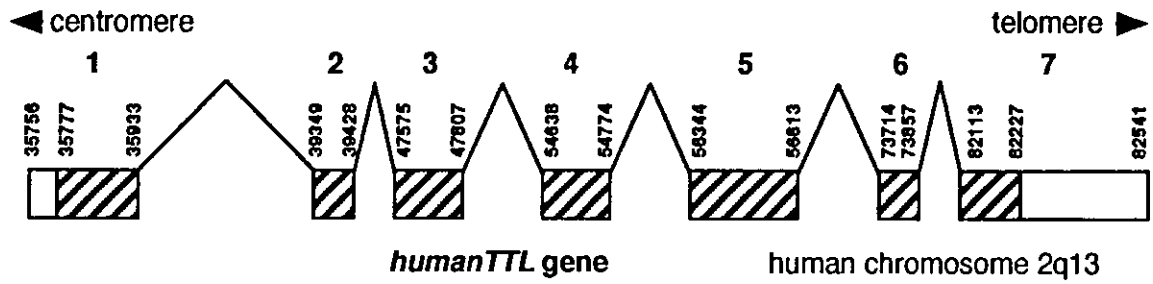

b

```
humanTTL  MYTFVVRDENSSVYAEVSRLLLATGHWKRLRRDNPRFNLMLGERNRLPFGRLGHEPGLVQLVNYYRGADKLCRKAS 76
mouseTTL  MYTFVVRDENSSVYAEVSRLLLATGYWKRLRRDNPRFNLMLGERNRLPFGRLGHEPGLAQLVNYYRGADKLCRKAS 76
ratTTL    MYTFVVRQENSSVYAEVSRLLLATGYWKRLRRDNPRFNLMLGGRNRLPFGRLGHEPGLAQLVNYYRGADKLCRKAS 76
pigTTL    MYTFVVRDENSSVYAEVSRLLLATGHWKRLRRDNPRFNLMLGERNRLPFGRLGHEPGLMQLVNYYRGADKLCRKAS 76
cowTTL    MYTFVVRDENSSVYAEVSRLLLATGHWKRLRRDNPRFNLMLGERNRLPFGRLGHEPGLMQLVNYYRGADKLCRKAS 76
          ******* ***************** ***************** ***************** ****************

humanTTL  LVKLIKTSPELAESCTWFPESYVIYPTNLKTPVAPAQNGIQPPISNSRTDEREFFLASYNRKKEDGEGNVWIAKSS 152
mouseTTL  LVKLVKTSPELSESCSWFPESYVIYPTNLKTPVAPAQNGIQLPVSNSRTDEREFFLASYNRKKEDGEGNVWIAKSS 152
ratTTL    LVKLVKTSPELSESCSWFPESYVIHPTNLKTPVAPAQNGIQLPVSNSRTDEREFFLASYNRKKEDGEGNVWIAKSS 152
pigTTL    LVKLIKTSPELAESCTWFPESYVIYPTNLKTPVAPAQNGIHPPIHSSRTDEREFFLTSYNKKKEDGEGNVWIAKSS 152
cowTTL    LVKLIKTSPELAESCTWFPESYVIYPTNLKTPVAPAQDGIHPPLHSSRTDEREFFLASYNRKKEEGEGNVWIAKSS 152
          **** ****** *** ******** ************ **  *   ********** *** *** ************

humanTTL  AGAKGEGILISSEASELLDFIDNQGQVHVIQKYLEHPLLLEPGHRKFDIRSWVLVDHQYNIYLYREGVLRTASEPY 228
mouseTTL  AGAKGEGILISSEASELLDFIDSQGQVHVIQKYLERPLLLEPGHRKFDIRSWVLVDHQYNIYLYREGVLRTASEPY 228
ratTTL    AGAKGEGILISSEASELLDFIDNQGQVHVIQKYLEHPLLLEPGHRKFDIRSWVLVDHQYNIYLYREGVLRTASEPY 228
pigTTL    AGAKGEGILISSEATELLDFIDNQGQVHVIQKYLERPLLLEPGHRKFDIRSWVLVDHQYNIYLYREGVLRTASEPY 228
cowTTL    AGAKGEGILISSDATELLDFIDNQGQVHVIQKYLERPLLLEPGHRKFDIRSWVLVDHQFNIYLYREGVLRTASEPY 228
          ************ * ******* ************ ********************** ****************

humanTTL  HVDNFQDKTCHLTNHCIQKEYSKNYGKYEEGNEMFFKEFNQYLTSALNITLESSILLQIKHIIRNCLLSVEPAIST 304
mouseTTL  HVDNFQDKTCHLTNHCIQKEYSKNYGKYEEGNEMFFEEFNQYLTSALNITLESSILLQIKHIIRSCLMSVEPAIST 304
ratTTL    HVDNFQDKTCHLTNHCIQKEYSKNYGKYEEGNEMFFEEFNQYLTSALNITLENSILLQIKHIIRSCLMSVEPAIST 304
pigTTL    HTDNFQDKTCHLTNHCIQKEYSKNYGKYEEGNEMFFEEFNQYLTSALNITLESSILLQIKHIIRSCLLSVEPAIST 304
cowTTL    HMDNFQDKTCHLTNHCIQKEYSKNYGKYEEGNEMFFEAFNRYLTSALNITLESSILLQIKHIIRSCLMSVEPAIST 304
          * ********************************** ** *********** *********** ** ********

humanTTL  KHLPYQSFQLFGFDFMVDEELKVWLIEVNGAPACAQKLYAELCQGIVDIAISSVFPPPDVEQPQTQP--AAFIKL 377
mouseTTL  KHLPYQSFQLLGFDFMVDEELKVWLIEVNGAPACAQKLYAELCQGIVDIAISSVFPPPDTEQVPQQP--AAFVKL 377
ratTTL    KHLPYQSFQLLGFDFMVDEELKVWLIEVNGAPACAQKLYAELCQGIVDIAISSVFPPPDTEQVPQQP--AAFMKL 377
pigTTL    RHLPYQSFQLFGFDFMVDEDLKVWLIEVNGAPACAQKLYAELCQGIVDIAIASVFPPPDAEQQQQQPPPAAFIKL 379
cowTTL    KHLPYQSFQLFGFDFMVDEELKVWLIEVNGAPACAQKLYAELCQGIVDIAIASVFPPPDAEQQPPQP--ATFIKL 377
          ********* ******** ********************************** ******* **   **  * * **
```

c

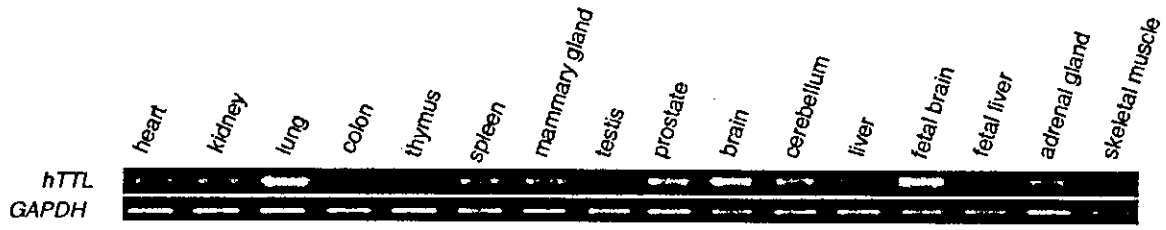

FIGURE 2

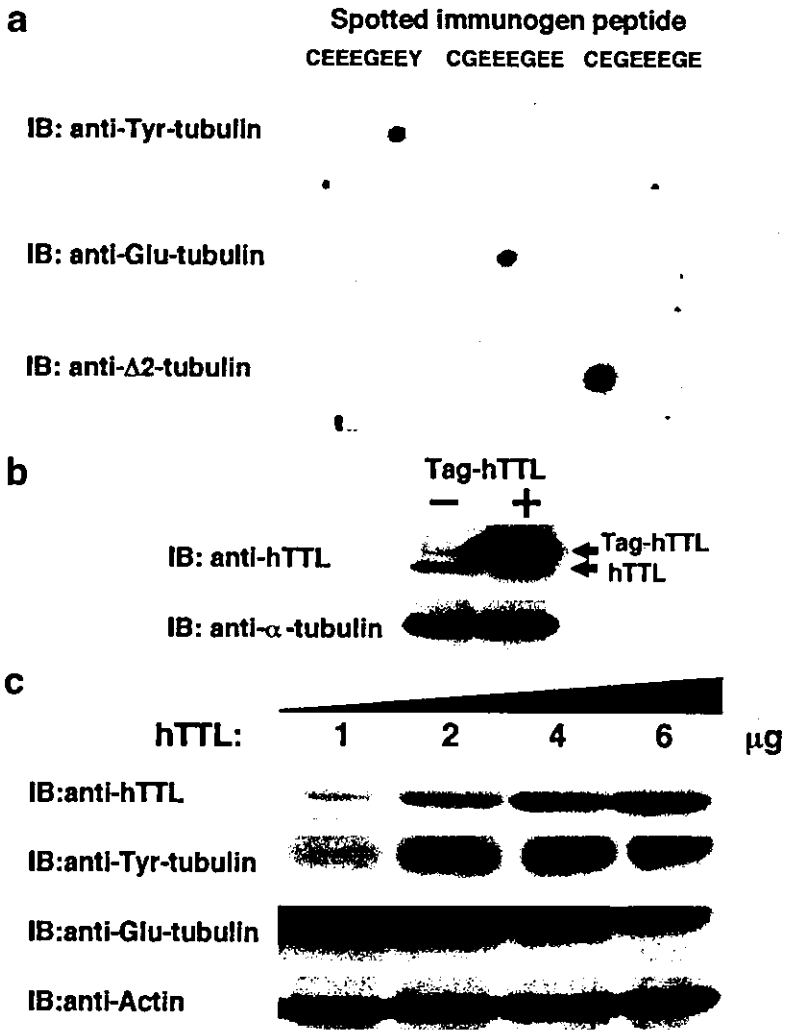

FIGURE 3 – hTTL has a tyrosination activity in mammalian cultured cells. (*a*) Specificity of antibodies. The indicated synthetic peptides were spotted on the filter and immunoblotted with the polyclonal anti-Tyr-tubulin (top), anti-Glu-tubulin (middle), or anti-Δ2-tubulin antibody (bottom). (*b*) Expression of FLAG-tagged hTTL. Whole-cell lysates prepared from COS7 cells transfected with the empty plasmid or with the expression plasmid for FLAG-tagged hTTL were subjected to immunoblotting with the anti-hTTL antibody (top). The expression level of α-tubulin was examined to ensure equal loading (bottom). (*c*) The exogenously expressed hTTL has a catalytic activity. HEK293T cells were transfected with increasing amounts of the hTTL expression plasmid. Forty-eight hours after transfection, whole-cell lysates were prepared and immunoblotted with the indicated antibodies. The expression level of actin is included as a loading control (bottom).

cells with 1 nM BMP2 or 5 μM RA induced remarkable morphologic differentiation by day 8. The hTTL protein level was increased after day 2 and peaked on day 6 in the former and on day 3 in the latter. Thereafter, it appeared to be decreased. Thus, hTTL was induced during induction of neuronal differentiation in NBL cells.

Expression of hTTL mRNA in primary neuroblastomas

To evaluate the clinical significance of *hTTL*, we examined the expression of *hTTL* mRNA in 16 favorable (stage 1, high expression of *TrkA* and a single copy of *MYCN*) and 16 unfavorable (stage 3 or 4, low expression of *TrkA* and amplification of *MYCN*) NBLs using semiquantitative RT-PCR. As shown in Figure 5(*a*), *hTTL* was preferentially expressed in favorable NBLs. Therefore, we next performed quantitative real-time RT-PCR to measure the levels of *hTTL* transcript in 74 primary NBLs. Table I shows the quantitative levels of *hTTL* mRNA expression (mean ± SEM) by age (< 1-year-old *vs.* ≥ 1-year-old), tumor stages (1 + 2 + 4s *vs.* 3 + 4), *TrkA* expression (low *vs.* high), *MYCN* gene copies (single *vs.* amplified), origin (adrenal gland *vs.* others), mass screening (tumors found by mass screening *vs.* sporadic tumors) and prognosis (alive *vs.* dead). High levels of *hTTL* expression were significantly associated with favorable stages ($p = 0.0069$), high *TrkA* expression ($p = 0.002$), a single copy of *MYCN* ($p < 0.00005$), tumors found by mass screening ($p = 0.0042$), origins other than adrenal gland ($p = 0.0042$) and a good prognosis ($p = 0.023$). *hTTL* expression was marginally associated with age. The log-rank test indicated that *hTTL* expression was associated with better survival ($p = 0.026$), which was also indicated in the Kaplan-Meier cumulative survival curves (Fig. 5*b*).

The univariate Cox regression was employed to examine the individual relationship of each variable to survival (Table II). Expression of *hTTL*, age, *MYCN* copy numbers and mass screening were found to be of prognostic importance, supporting the results of the log-rank test. However, since *hTTL* expression was highly associated with *MYCN*, mass screening and origin, multivariable Cox models were not fitted to assess the predictive importance of *hTTL* expression for survival after controlling these prognostic factors, suggesting that expression of *hTTL* was not an independent prognostic indicator.

FIGURE 2 – Genomic structure, alignment of amino acid sequence and mRNA expression of human *TTL*. (*a*) Genomic structure of *hTTL*. The *hTTL* gene that is mapped to 2q13 consists of 7 exons. Untranslated regions (open boxes) and coding regions (hatched boxes) are shown. Numbers indicate nucleotide position in human BAC clone *RP11-1124* (accession number AC012442). (*b*) Comparison of amino acid sequences among mammalian TTLs. The gaps produced by the alignment are indicated by a hyphen in the sequence. The conserved amino acid residues in TTLs are shown by asterisks below the alignment. (*c*) Tissue distribution of *hTTL* mRNA. The expression levels of *hTTL* mRNA in the indicated human tissues were examined by semiquantitative RT-PCR (top). *GAPDH* expression was also examined as an internal control (bottom).

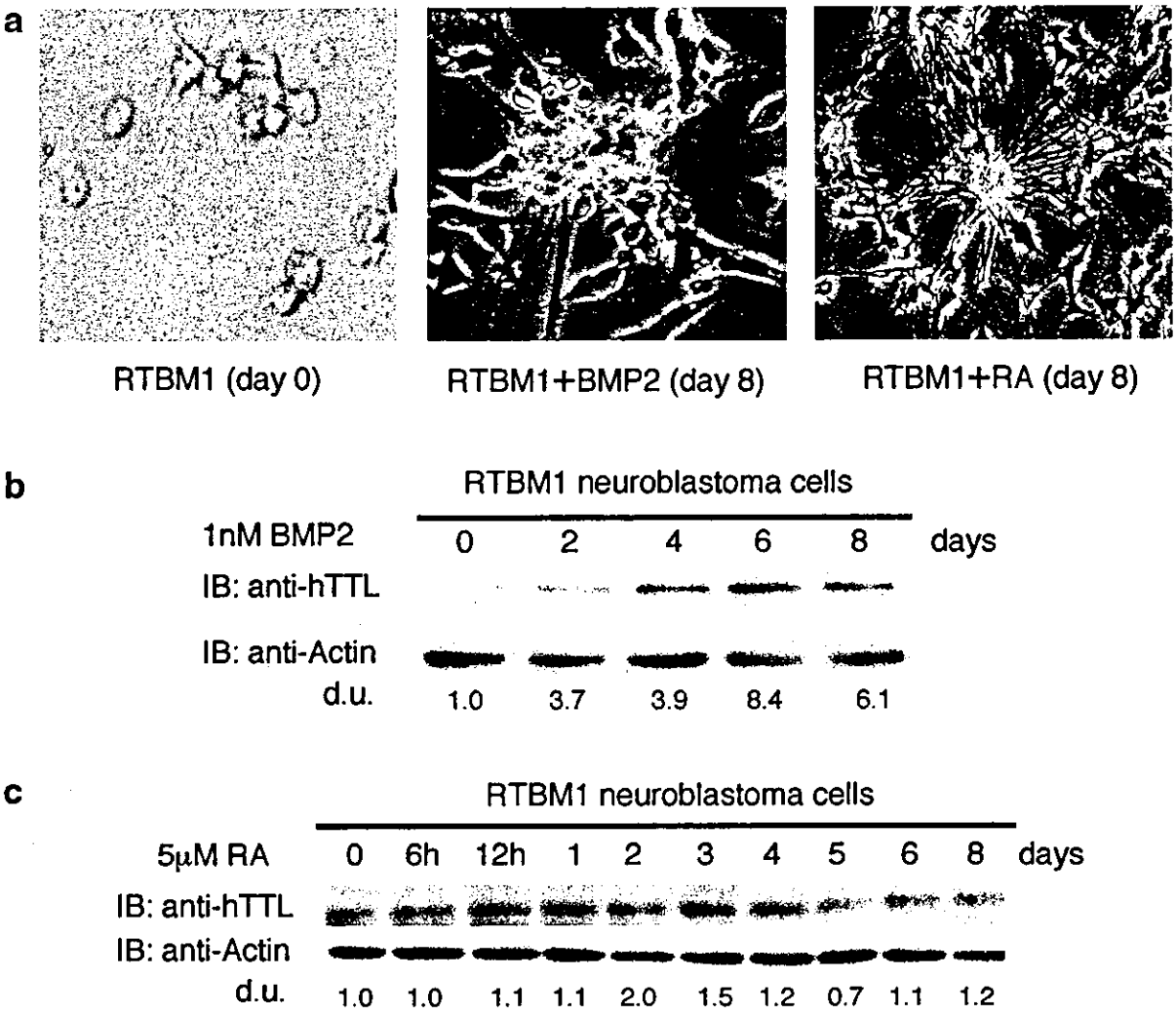

FIGURE 4 – TTL is induced during BMP2- and RA-mediated neuroblastoma differentiation. (*a*) BMP2- or RA-induced morphologic changes in RTBM1 neuroblastoma cells. RTBM1 cells were treated with BMP2 or RA at a final concentration of 1 nM or 5 μM, respectively, and maintained for 8 days. (*b*) Expression levels of hTTL are increased in response to BMP2. At the indicated time points after the treatment with BMP2 (at a final concentration of 1 nM), whole-cell lysates prepared from RTBM1 cells were subjected to immunoblotting with the antibody against hTTL (top). Actin protein levels were determined as a loading control (bottom). (*c*) Induction of hTTL in response to RA. RTBM1 cells were exposed to RA at a final concentration of 5 μM. Whole-cell lysates were prepared at the indicated time points after the treatment with RA and subjected to immunoblotting with the anti-hTTL (top) or with antiactin (bottom) antibody. d.u., arbitrary density units.

Immunohistochemistry

To determine the expression pattern of hTTL protein in primary NBLs, we performed immunohistochemical study for 6 favorable (stage 1 or 2 and a single copy of *MYCN*) and 4 unfavorable (stage 3 or 4 and amplified *MYCN*) NBLs. hTTL, Tyr-tubulin and Glu-tubulin were positively detected both in the cytoplasm of the neuroblastic cells and in the fine meshwork of neuropil of all 6 tumors with favorable histology (Shimada's classification) and a single copy of *MYCN* (Fig. 6*a–c*). In contrast, all 4 tumors with unfavorable histology and *MYCN* amplification were negative for Tyr-tubulin and Glu-tubulin, and only 1 tumor in this subset was positive for hTTL (Fig. 6*f–h*). Interestingly, all 10 NBL tumors were positive for Δ2-tubulin, but whose staining pattern was rather distinct in different subsets of the tumors. In the favorable tumors, Δ2-tubulin showed a localization similar to hTTL, Tyr-tubulin and Glu-tubulin and was detected in the cytoplasm and in the fine neuropil (Fig. 6*d*). On the other hand, Δ2-tubulin in the aggressive tumors was found only in the cytoplasm of neuroblastic cells, since they had no or a very limited capability of neuritic process production (*i.e.*, neuropil formation; Fig. 6*i*).

CD56 was detected in all 10 tumors, regardless of the histology and *MYCN* status (data not shown). TrkA was detected in all of 6 favorable tumors (Fig. 6*e*), but was negative in 3 of 4 aggressive tumors (Fig. 6*j*). It was noted that one unfavorable tumor with weakly positive trkA showed positive staining for TTL. Ki-67 staining revealed 10–20% and 60–70% positive cells in the favorable and the unfavorable tumors, respectively (data not shown).

DISCUSSION

In the present study, we have identified human ortholog of *tubulin tyrosine ligase* gene, which is highly conserved among the mammalian species. *hTTL* mRNA is ubiquitously expressed but rather preferential in both fetal and adult brains as well as in lung. The specific antibodies raised against hTTL, Tyr-tubulin, Glu-tubulin and Δ2-tubulin have confirmed the catalytic activity of

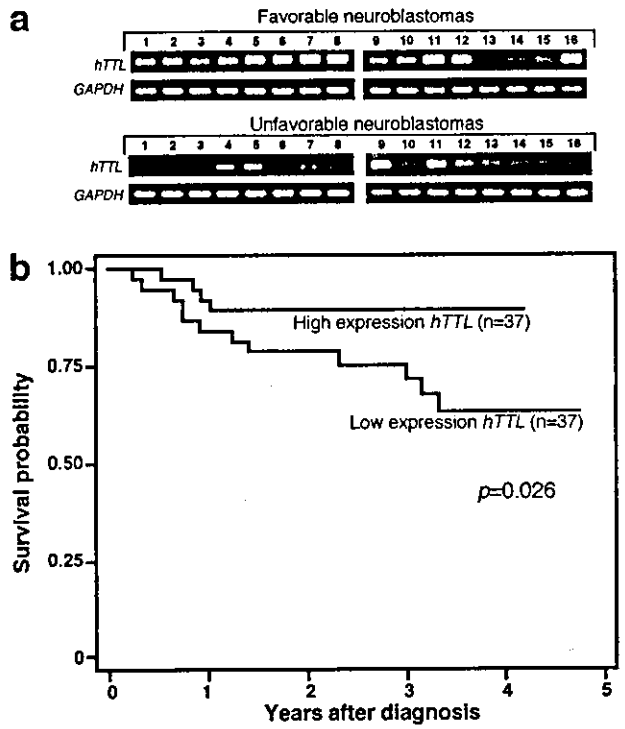

FIGURE 5 – Expression of *hTTL* mRNA is associated with unfavorable prognosis of neuroblastoma. (*a*) Total RNA was purified from the indicated favorable (top) and unfavorable NBL tissues (bottom) and subjected to semiquantitative RT-PCR. Sixteen favorable cases used in this study were classified as stage 1 NBL with a single copy *MYCN* as well as a high expression of *TrkA*. Sixteen unfavorable cases were in stages 3 and 4 NBL with *MYCN* amplification as well as a low *TrkA* expression. *GAPDH* expression was also examined as an internal control. (*b*) Association of *hTTL* mRNA expression levels with favorable prognosis of NBL. Total RNA was prepared from 74 NBL tissues, and *hTTL* mRNA levels were assayed by quantitative real-time RT-PCR as described in text. The values of *hTTL* mRNA were normalized by *GAPDH*. The survival of *hTTL* relatively high-expression group (n = 37) and *hTTL* low-expression group (n = 37) was compared using the Kaplan-Meier procedure.

TABLE I – RESULTS OF LOG-RANK TESTS FOR CONVENTIONAL PROGNOSTIC FACTORS AND EXPRESSION OF *hTTL* IN 74 PRIMARY NEUROBLASTOMAS

Variable	n	*hTTL* expression[1]	p-value
Age (year)			0.1
<1	43	117 ± 14	
≥1	31	77 ± 10	
Tumor stage			0.0069
1, 2, 4s	40	127 ± 14	
3, 4	34	69 ± 9	
TrkA expression			0.002
High	36	125 ± 17	
Low	38	77 ± 8	
MYCN			<0.00005
Single	52	123 ± 11	
Amplified	22	46 ± 9	
Mass screening			0.0042
+	37	128 ± 14	
−	37	72 ± 10	
Origin			0.0042
Adrenal gland	47	85 ± 11	
Others	27	127 ± 16	
Prognosis			0.023
Alive	58	113 ± 11	
Dead	16	54 ± 11	

[1]Mean ± SEM.

TABLE II – COX REGRESSION MODELS USING DICHOTOMOUS FACTORS OF AGE, *MYCN* AMPLIFICATION, MASS SCREENING, ORIGIN AND EXPRESSION OF *hTTL*

Factor	p-value	Hazard ratio (95% confidence interval)
hTTL expression (log)	0.024	0.64 (0.44, 0.94)
Age (> 1 *vs.* < 1 year)	0.005	5.04 (1.61, 15.8)
MYCN (1 copy *vs.* > 1 copy)	<0.0005	0.06 (0.017, 0.22)
Mass screening (+ *vs.* −)	0.004	0.05 (0.007, 0.38)
Origin (adrenal gland *vs.* others)	0.31	1.79 (0.58, 5.57)

hTTL encoded by the *hTTL* gene in the cells. Interestingly, hTTL is induced during neurite extension in RTBM1 NBL cells treated with BMP2 or RA, suggesting that hTTL expression is associated with neuronal differentiation in human NBL. Immunohistochemically, favorable NBLs are positive for hTTL, Tyr-tubulin, Glu-tubulin and Δ2-tubulin, whereas unfavorable tumors with *MYCN* amplification are positive only for Δ2-tubulin, suggesting that deregulation of tyrosination/detyrosination cycle contributes to malignant progression of NBL. This hypothesis has been further supported by a significant decrease of the levels of *hTTL* expression in the patients with poor prognosis.

The dynamics of microtubule regulates many cellular functions, including migration, motility, differentiation, cell division and cellular cap formation. Though posttranslational modifications of tubulin and their enzymatic regulation have long been studied, the precise mechanisms are still largely unknown. It is interesting that no orthologs of highly conserved mammalian TTL have so far been reported in *Caenorhabditis elegans*, *Drosophila melanogaster* and *Saccharomyces cerevisiae*, suggesting that the tyrosination/detyrosination cycle of tubulin may be related to evolution of the cellular functions, including neuronal differentiation. In newborn rats, TTL expression is found in skeletal muscle at high levels and is developmentally regulated by rapidly decreasing its level during early postnatal period.[31] It is interesting that both BMP2 and RA, which have increased levels of hTTL expression, function as regulators to induce differentiation during neural development.

The tyrosination/detyrosination of tubulin may be regulated by the activities of both TTL and tubulin carboxypeptidase (TCP). Until now, however, the *TCP* gene has never been identified in vertebrates, although biochemical TCP activity has been reported to be present in some subcellular fractions.[18] Tubulin is also posttranslationally modified by nitrotyrosination. Eiserich *et al.*[32] showed that free 3-nitrotyrosine (NO_2Tyr) is transported into mammalian cells and selectively incorporated into the Glu-tubulin posttranslationally, which is catalyzed by TTL. Cellular injury such as microtubule disorganization has consequently been induced. Kalisz *et al.*[33] also showed that nitrotyrosine can be incorporated into α-tubulin by *in vitro* assays. Those reports demonstrated that carboxypeptidase A is incapable of cleaving nitrotyrosine from the modified α-tubulin. On the other hand, Bisig *et al.*[34] reported that nitrotyrosinated tubulin is a good substrate of physiologic TCP, and that it has a similar capability to that of the tyrosinated tubulin to assemble into microtubules, suggesting that incorporation of nitrotyrosine is not injurious at least to dividing cells. Therefore, whether nitrotyrosinated tubulin is harmful or not is still controversial. Nevertheless, as increased nitrotyrosination is reported in Alzheimer's disease and amyotrophic lateral sclerosis,[35-37] the functional analysis of the role of hTTL and tubulin tyrosination/detyrosination cycle should be important for understanding the pathogenesis of these disease. The treatment of cells with methylmercury (MeHg) is also reported to induce perturbation of cellular activities associated with the tubulin/microtubule system by altering the status of tubulin tyrosination in the rat

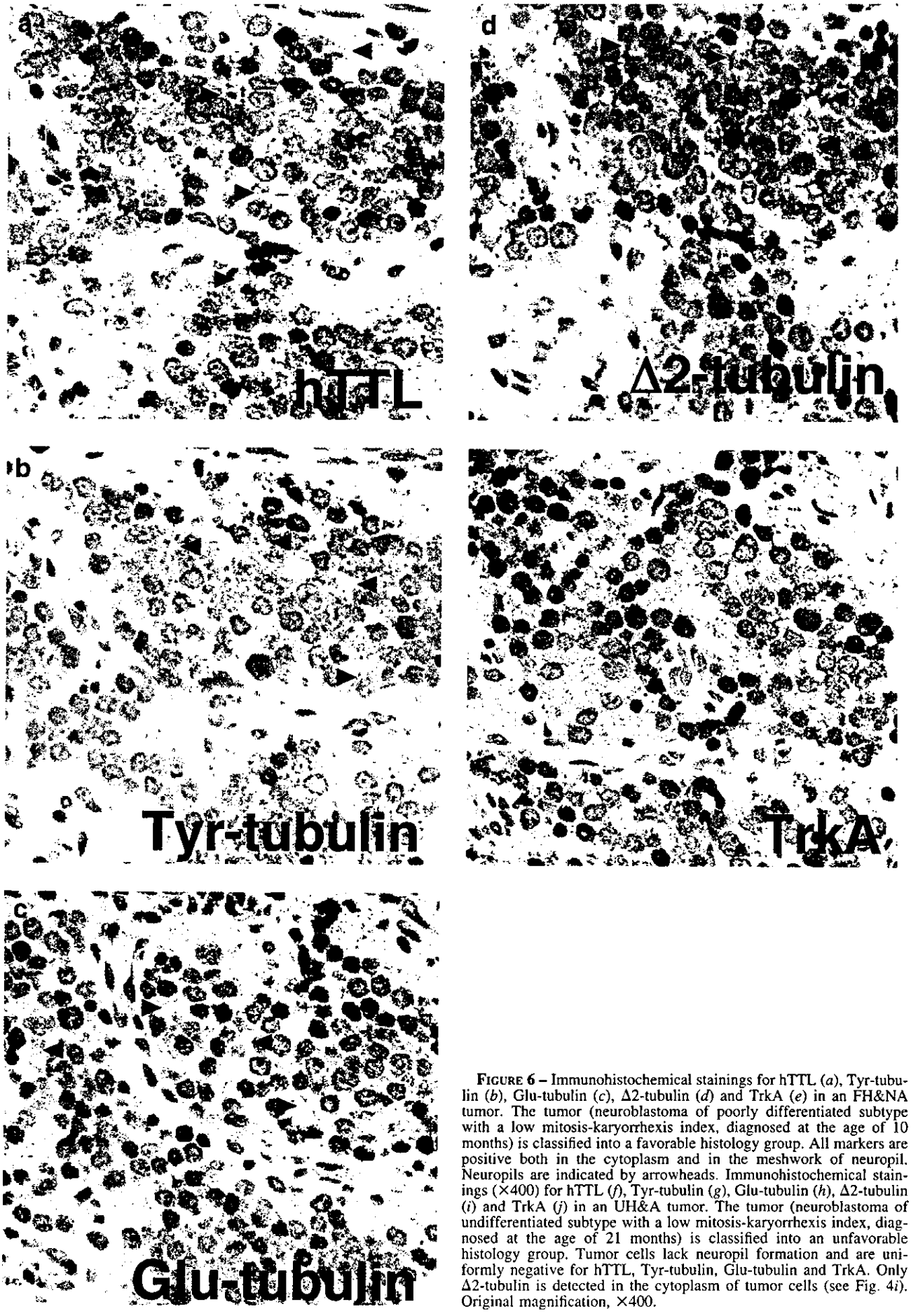

FIGURE 6 – Immunohistochemical stainings for hTTL (*a*), Tyr-tubulin (*b*), Glu-tubulin (*c*), Δ2-tubulin (*d*) and TrkA (*e*) in an FH&NA tumor. The tumor (neuroblastoma of poorly differentiated subtype with a low mitosis-karyorrhexis index, diagnosed at the age of 10 months) is classified into a favorable histology group. All markers are positive both in the cytoplasm and in the meshwork of neuropil. Neuropils are indicated by arrowheads. Immunohistochemical stainings (×400) for hTTL (*f*), Tyr-tubulin (*g*), Glu-tubulin (*h*), Δ2-tubulin (*i*) and TrkA (*j*) in an UH&A tumor. The tumor (neuroblastoma of undifferentiated subtype with a low mitosis-karyorrhexis index, diagnosed at the age of 21 months) is classified into an unfavorable histology group. Tumor cells lack neuropil formation and are uniformly negative for hTTL, Tyr-tubulin, Glu-tubulin and TrkA. Only Δ2-tubulin is detected in the cytoplasm of tumor cells (see Fig. 4*i*). Original magnification, ×400.

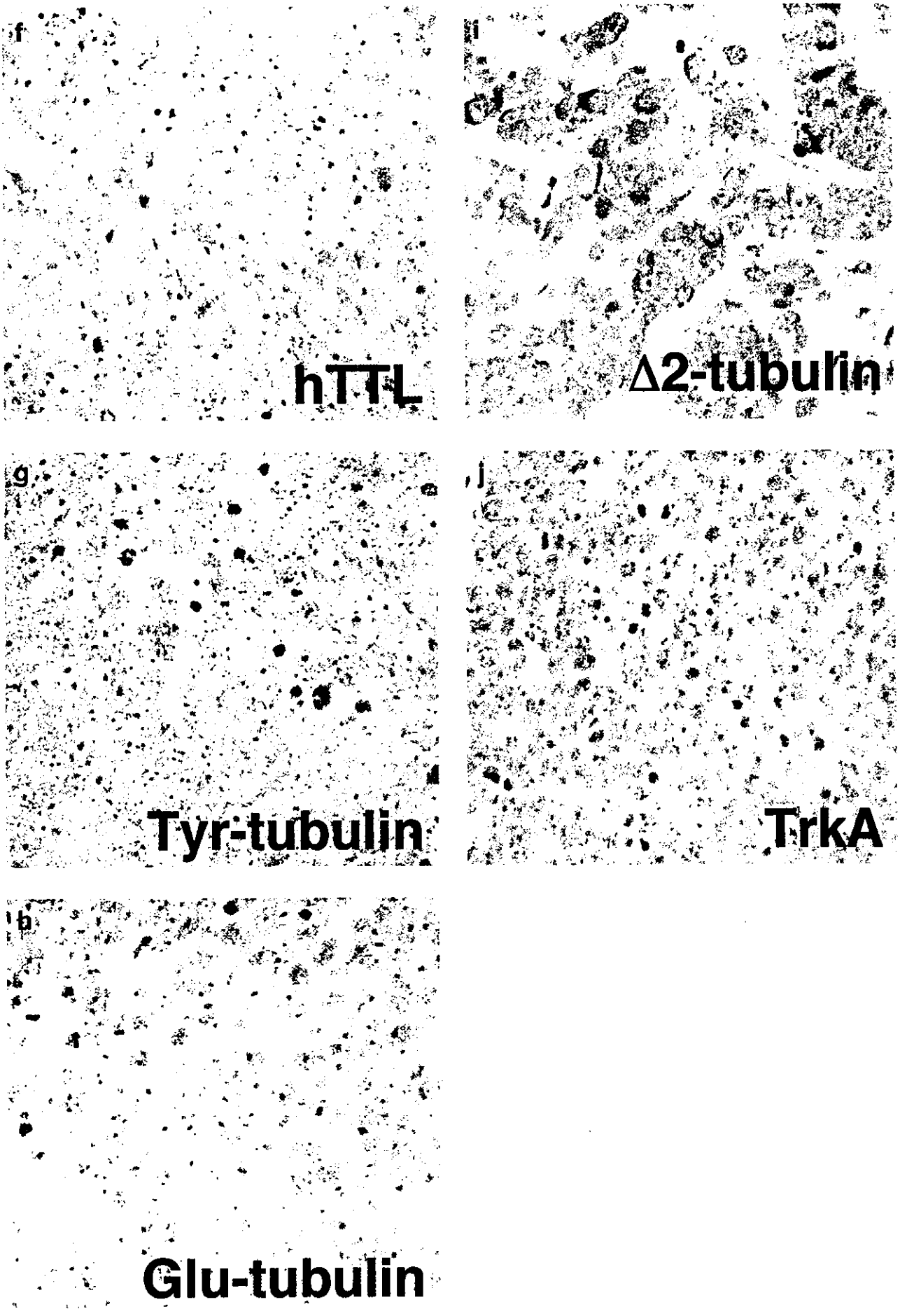

FIGURE 6 – (CONTINUED)

brain.[38] Therefore, many cellular stresses such as oxidative damage may trigger dysfunction of the tubulin/microtubule cytoskeletal system.

Our present study has shown that the decreases in Tyr-tubulin and Glu-tubulin are associated with relatively low levels of hTTL expression in unfavorable NBLs, which have lost a potency of neuronal differentiation and/or apoptosis. They are also correlated with decreased levels of TrkA, a high-affinity receptor for nerve growth factor, whose activation induces morphologic differentiation of NBL cells.[39] In addition, gradual upregulation of hTTL has been observed during induction of neuronal differentiation in RTBM1 cells treated with BMP2 or RA. These suggest that the induction of neuronal differentiation in NBL is accompanied with the activated tyrosination/detyrosination cycle regulated by increased level of hTTL enzyme, while the cycle is arrested by downregulation of hTTL in proliferating NBL cells, resulting in accumulation of Δ2-tubulin within the cells. Indeed, the expression levels of *hTTL* mRNA and Δ2-tubulin are significantly correlated with the prognosis of primary NBLs. This is consistent with the observation that TTL activity is lost, and conversely Δ2-tubulin is upregulated during the tumor cell growth.[19] Lafanechere *et al.*[19] have demonstrated by using mouse TTL null cells both *in vitro* and *in vivo* that mouse TTL activity is strongly decreased during tumor growth. Mas *et al.*[15] have also reported that, using rat *TTL* dominant negative mutant and an antisense cDNA of rat *TTL*, suppression of TTL activity induces 2- to 3-fold faster cell proliferation. Moreover, in human breast cancers, the accumulation of Glu-tubulin and Δ2-tubulin is correlated with poor prognosis by immunohistochemical approach.[28] It is noteworthy that our preliminary data using the microarray hybridized with total RNA obtained from 136 primary NBLs have shown that the gene with the highest score to predict prognosis of NBLs is α-tubulin (data not shown). Thus, the role of microtubule and its component, α-tubulin, is very important to define the biology as well as the aggressiveness of cancer cells.

In conclusion, we have identified a *human tubulin tyrosine ligase* gene and demonstrated its tissue distribution and correlation with neuronal differentiation. Since our data have suggested that the tyrosination cycle of α-tubulin is activated in differentiating NBLs but is inactivated in proliferating tumors, the cycle-related molecules including hTTL could be the targets for developing novel therapeutic strategies against advanced stages of NBL.

ACKNOWLEDGEMENTS

The authors thank Shigeru Sakiyama for critical reading of the manuscript, Naoko Sugimitsu for preparing RNA, Yuki Nakamura for DNA sequencing, Yoshiaki Okamoto for instructing quantitative real-time RT-PCR and Aiko Morohashi and Natsue Akao for technical assistance. The authors also thank the following institutions for providing surgical samples: First Department of Surgery, Hokkaido University School of Medicine; Department of Pediatrics, National Sapporo Hospital; Department of Pediatric Surgery, Tohoku University School of Medicine; Department of Surgery, Gunma Children's Medical Center; Department of Pediatrics, Pediatric Surgery and General Surgery, Jichi Medical University; Department of Hematology and Oncology, Saitama Children's Medical Center; Department of Pediatrics, Juntendo University School of Medicine; Department of Surgery, Kiyose Metropolitan Children's Hospital; Department of Surgery and Pathology, Chiba Children's Hospital; Department of Pediatric Surgery, Chiba University School of Medicine; Department of Pediatric Surgery, Kimitsu Central Hospital; Department of Pediatric Surgery, Niigata University School of Medicine; Department of Pediatrics and Pediatric Surgery, Aichi Medical University; Department of Pediatrics, Kyoto Prefectural Medical University; Tumor Board, Hyogo Children's Hospital; Department of Pediatrics and Pediatric Surgery, Kagoshima University School of Medicine; Department of Pediatric Surgery, Showa University School of Medicine; Department of Pediatrics, Oita University School of Medicine; Department of Pediatric Surgery, Ohta General Hospital; Department of Pediatrics, Ichinomiya City Hospital; Department of Pediatric Surgery, Osaka City General Hospital; Department of Pediatrics, Nihon University School of Medicine; Itabashi Hospital; Department of Pediatric Surgery, University of Tsukuba School of Medicine.

REFERENCES

1. MacRae TH. Tubulin post-translational modifications: enzymes and their mechanisms of action. Eur J Biochem 1997;244:265–78.
2. Zambito AM, Wolff J. Palmitoylation of tubulin. Biochem Biophys Res Commun 1997;239:650–4.
3. Barra HS, Arce CA, Argarana CE. Posttranslational tyrosination/detyrosination of tubulin. Mol Neurobiol 1988;2:133–53.
4. Luduena RF. Multiple forms of tubulin: different gene products and covalent modifications. Int Rev Cytol 1998;178:207–75.
5. Barra HS, Unates LE, Sayavedra MS, Caputto R. Capacities for binding amino acids by tRNAs from rat brain and their changes during development. J Neurochem 1972;19:2289–97.
6. Barra HS, Rodriguez JA, Arce CA, Caputto R. A soluble preparation from rat brain that incorporates into its own proteins (14 C)arginine by a ribonuclease-sensitive system and (14 C)tyrosine by a ribonuclease-insensitive system. J Neurochem 1973;20:97–108.
7. Barra HS, Arce CA, Rodriguez JA, Caputto R. Incorporation of phenylalanine as a single unit into rat brain protein: reciprocal inhibition by phenylalanine and tyrosine of their respective incorporations. J Neurochem 1973;21:1241–51.
8. Barra HS, Arce CA, Rodriguez JA, Caputto R. Some common properties of the protein that incorporates tyrosine as a single unit and the microtubule proteins. Biochem Biophys Res Commun 1974;60:1384–90.
9. Arce CA, Rodriguez JA, Barra HS, Caputo R. Incorporation of L-tyrosine, L-phenylalanine and L-3,4-dihydroxyphenylalanine as single units into rat brain tubulin. Eur J Biochem 1975;59:145–9.
10. Argarana CE, Arce CA, Barra HS, Caputto R. *In vivo* incorporation of [14C]tyrosine into the C-terminal position of the alpha subunit of tubulin. Arch Biochem Biophys 1977;180:264–8.
11. Preston SF, Deanin GG, Hanson RK, Gordon MW. The phylogenetic distribution of tubulin:tyrosine ligase. J Mol Evol 1979;13:233–44.
12. Gabius HJ, Graupner G, Cramer F. Activity patterns of aminoacyl-tRNA synthetases, tRNA methylases, arginyltransferase and tubulin: tyrosine ligase during development and ageing of *Caenorhabditis elegans*. Eur J Biochem 1983;131:231–4.
13. Stieger J, Wyler T, Seebeck T. Partial purification and characterization of microtubular protein from *Trypanosoma brucei*. J Biol Chem 1984;259:4596–602.
14. Ersfeld K, Wehland J, Plessmann U, Dodemont H, Gerke V, Weber K. Characterization of the tubulin-tyrosine ligase. J Cell Biol 1993;120:725–32.
15. Mas CR, Arregui CO, Filiberti A, Argarana CE, Barra HS. Cloning of rat olfactory bulb tubulin tyrosine ligase cDNA: a dominant negative mutant and an antisense cDNA increase the proliferation rate of cells in culture. Neurochem Res 2002;27:1453–8.
16. Paturle-Lafanechere L, Edde B, Denoulet P, Van Dorsselaer A, Mazarguil H, Le Caer JP, Wehland J, Job D. Characterization of a major brain tubulin variant which cannot be tyrosinated. Biochemistry 1991;30:10523–8.
17. Paturle-Lafanechere L, Manier M, Trigault N, Pirollet F, Mazarguil H, Job D. Accumulation of delta 2-tubulin, a major tubulin variant that cannot be tyrosinated, in neuronal tissues and in stable microtubule assemblies. J Cell Sci 1994;107:1529–43.
18. Lafanechere L, Job D. The third tubulin pool. Neurochem Res 2000;25:11–8.
19. Lafanechere L, Courtay-Cahen C, Kawakami T, Jacrot M, Rudiger M, Wehland J, Job D, Margolis RL. Suppression of tubulin tyrosine ligase during tumor growth. J Cell Sci 1998;111:171–81.
20. Ohira M, Morohashi A, Inuzuka H, Shishikura T, Kawamoto T, Kageyama H, Nakamura Y, Isogai E, Takayasu H, Sakiyama S, Suzuki Y, Sugano S, Goto T, Sato S, Nakagawara A. Expression profiling and characterization of 4200 genes cloned from primary neuroblastomas: identification of 305 genes differentially expressed between favorable and unfavorable subsets. Oncogene 2003;22:5525–36.
21. Ohira M, Morohashi A, Nakamura Y, Isogai E, Furuya K, Hamano S, Machida T, Aoyama M, Fukumura M, Miyazaki K, Suzuki Y, Sugano S, Hirato J, Nakagawara A. Neuroblastoma oligo-capping cDNA

project: toward the understanding of the genesis and biology of neuroblastoma. Cancer Lett 2003;197:63–8.
22. Brodeur GM, Pritchard J, Berthold F, Carlsen NL, Castel V, Castelberry RP, De Bernardi B, Evans AE, Favrot M, Hedborg F, kaneko M, Kemshead J, Lampert F, Lee RE, Look AT, Pearson AD, Philip T, Roald B, Sawada T, Seeger RC, Thuchida Y, Voute PA. Revisions of the international criteria for neuroblastoma diagnosis, staging, and response to treatment. J Clin Oncol 1993;11:1466–77.
23. Kaneko M, Nishihira H, Mugishima H, Ohnuma N, Nakada K, Kawa K, Fukuzawa M, Suita S, Sera Y, Tsuchida Y. Stratification of treatment of stage 4 neuroblastoma patients based on N-myc amplification status: Study Group of Japan for Treatment of Advanced Neuroblastoma, Tokyo, Japan. Med Pediatr Oncol 1998;31:1–7.
24. Hishiki T, Nimura Y, Isogai E, Kondo K, Ichimiya S, Nakamura Y, Ozaki T, Sakiyama S, Hirose M, Seki N, Takahashi H, Ohnuma N, Tanabe M, Nakagawara A. Glial cell line-derived neurotrophic factor/neurturin-induced differentiation and its enhancement by retinoic acid in primary human neuroblastomas expressing c-Ret, GFR alpha-1, and GFR alpha-2. Cancer Res 1998;58:2158–65.
25. Chomczynski P, Sacchi N. Single-step method of RNA isolation by acid guanidinium thiocyanate-phenol-chloroform extraction. Anal Biochem 1987;162:156–9.
26. Shimada H, Ambros IM, Dehner LP, Hata J, Joshi VV, Roald B, Stram DO, Gerbing RB, Lukens JN, Matthay KK, Castleberry RP. The International Neuroblastoma Pathology Classification (the Shimada system). Cancer 1999;86:364–72.
27. Goto S, Umehara S, Gerbing RB, Stram DO, Brodeur GM, Seeger RC, Lukens JN, Matthay KK, Shimada H. Histopathology (International Neuroblastoma Pathology Classification) and MYCN status in patients with peripheral neuroblastic tumors: a report from the Children's Cancer Group. Cancer 2001;92:2699–708.
28. Mialhe A, Lafanechere L, Treilleux I, Peloux N, Dumontet C, Bremond A, Panh MH, Payan R, Wehland J, Margolis RL, Job D. Tubulin detyrosination is a frequent occurrence in breast cancers of poor prognosis. Cancer Res 2001;61:5024–7.
29. Iwasaki S, Hattori A, Sato M, Tsujimoto M, Kohno M. Characterization of the bone morphogenetic protein-2 as a neurotrophic factor: induction of neuronal differentiation of PC12 cells in the absence of mitogen-activated protein kinase activation. J Biol Chem 1996;271:17360–5.
30. Nakamura Y, Ozaki T, Koseki H, Nakagawara A, Sakiyama S. Accumulation of p27 KIP1 is associated with BMP2-induced growth arrest and neuronal differentiation of human neuroblastoma-derived cell lines. Biochem Biophys Res Commun 2003;307:206–13.
31. Arregui CO, Mas CR, Argarana CE, Barra HS. Tubulin tyrosine ligase: protein and mRNA expression in developing rat skeletal muscle. Dev Growth Differ 1997;39:167–78.
32. Eiserich JP, Estevez AG, Bamberg TV, Ye YZ, Chumley PH, Beckman JS, Freeman BA. Microtubule dysfunction by posttranslational nitrotyrosination of alpha-tubulin: a nitric oxide-dependent mechanism of cellular injury. Proc Natl Acad Sci USA 1999;96:6365–70.
33. Kalisz HM, Erck C, Plessmann U, Wehland J. Incorporation of nitrotyrosine into alpha-tubulin by recombinant mammalian tubulin-tyrosine ligase. Biochim Biophys Acta 2000;1481:131–8.
34. Bisig CG, Purro SA, Contin MA, Barra HS, Arce CA. Incorporation of 3-nitrotyrosine into the C-terminus of alpha-tubulin is reversible and not detrimental to dividing cells. Eur J Biochem 2002;269:5037–45.
35. Ischiropoulos H. Biological tyrosine nitration: a pathophysiological function of nitric oxide and reactive oxygen species. Arch Biochem Biophys 1998;3561–611.
36. Hensley K, Maidt ML, Yu Z, Sang H, Markesbery WR, Floyd RA. Electrochemical analysis of protein nitrotyrosine and dityrosine in the Alzheimer brain indicates region-specific accumulation. J Neurosci 1998;18:8126–32.
37. Beal MF, Ferrante RJ, Browne SE, Matthews RT, Kowall NW, Brown RH Jr. Increased 3-nitrotyrosine in both sporadic and familial amyotrophic lateral sclerosis. Ann Neurol 1997;42:644–54.
38. Ishida Y, Ichimura T, Sumi H, Horigome T, Omata S. Methylmercury alters the tyrosination status of tubulin in the brains of acutely intoxicated rats. Toxicology 1997;122:171–81.
39. Nakagawara A, Arima-Nakagawara M, Scavarda NJ, Azar CG, Cantor AB, Brodeur GM. Association between high levels of expression of the TRK gene and favorable outcome in human neuroblastoma. N Engl J Med 1993;328:847–54.

Oncogene (2004) 23, 5901–5911

www.nature.com/onc

Expression profiling and differential screening between hepatoblastomas and the corresponding normal livers: identification of high expression of the *PLK1* oncogene as a poor-prognostic indicator of hepatoblastomas

Shin-ichi Yamada[1], Miki Ohira[1], Hiroshi Horie[2], Kiyohiro Ando[1], Hajime Takayasu[1], Yutaka Suzuki[3], Sumio Sugano[3], Takahiro Hirata[4], Takeshi Goto[4], Tadashi Matsunaga[2], Eiso Hiyama[2], Yutaka Hayashi[2], Hisami Ando[2], Sachiyo Suita[2], Michio Kaneko[2], Fumiaki Sasaki[2], Kohei Hashizume[2], Naomi Ohnuma[2] and Akira Nakagawara*[,1,2]

[1]*Division of Biochemistry, Chiba Cancer Center Research Institute, Chiba 260-8717, Japan;* [2]*Japanese Study Group for Pediatric Liver Tumor, Japan;* [3]*Human Genome Center, Institute of Medical Science, University of Tokyo, Tokyo 108-8639, Japan;* [4]*Hisamitsu Pharmaceutical Co. Inc., Tokyo 100-6221, Japan*

Hepatoblastoma is one of the most common malignant liver tumors in young children. Recent evidences have suggested that the abnormalities in Wnt signaling pathway, as seen in frequent mutation of the *β-catenin* gene, may play a role in the genesis of hepatoblastoma. However, the precise mechanism to cause the tumor has been elusive. To identify novel hepatoblastoma-related genes for unveiling the molecular mechanism of the tumorigenesis, a large-scale cloning of cDNAs and differential screening of their expression between hepatoblastomas and the corresponding normal livers were performed. We constructed four full-length-enriched cDNA libraries using an oligo-capping method from the primary tissues which included two hepatoblastomas with high levels of alpha-fetoprotein (AFP), a hepatoblastoma without production of AFP, and a normal liver tissue corresponded to the tumor. Among the 10431 cDNAs randomly picked up and successfully sequenced, 847 (8.1%) were the genes with unknown function. Of interest, the expression profile among the two subsets of hepatoblastoma and a normal liver was extremely different. A semiquantitative RT–PCR analysis showed that 86 out of 1188 genes tested were differentially expressed between hepatoblastomas and the corresponding normal livers, but that only 11 of those were expressed at high levels in the tumors. Notably, *PLK1* oncogene was expressed at very high levels in hepatoblastomas as compared to the normal infant's livers. Quantitative real-time RT–PCR analysis for the *PLK1* mRNA levels in 74 primary hepatoblastomas and 29 corresponding nontumorous livers indicated that the patients with hepatoblastoma with high expression of *PLK1* represented significantly poorer outcome than those with its low expression (5-year survival rate: 55.9 vs 87.0%, respectively, $p = 0.042$), suggesting that the level of *PLK1* expression is a novel marker to predict the prognosis of hepatoblastoma. Thus, the differentially expressed genes we have identified may become a useful tool to develop new diagnostic as well as therapeutic strategies of hepatoblastoma.
Oncogene (2004) **23**, 5901–5911. doi:10.1038/sj.onc.1207782
Published online 28 June 2004

Keywords: hepatoblastoma; expression profile; oligo-capping cDNA library; PLK1; prognostic factor

Introduction

Hepatoblastoma (HBL) is the most common hepatic cancer in children (Exelby *et al.*, 1975; Weinberg and Finegold, 1983). However, the etiology of HBL has been unclear in contrast to the adult hepatocellular carcinoma (HCC), in which preceding infection of hepatitis virus is often found (Buendia, 1992; Idilman *et al.*, 1998). Although most HBLs are sporadic, it is sometimes associated with certain hereditary diseases such as Beckwith–Wiedemann syndrome (Albrecht *et al.*, 1994) and familial adenomatous polyposis (Li *et al.*, 1987; Giardiello *et al.*, 1996; Kinzler and Vogelstein, 1996). In the former, loss of heterozygosity of chromosome 11p15.5 is frequently observed, and the abnormal regulation of the *insulin-like growth factor 2* (*IGF2*) and the *H19* genes at this locus may contribute to the disease (Albrecht *et al.*, 1994; Montagna *et al.*, 1994; Li *et al.*, 1995; Rainier *et al.*, 1995; Yun *et al.*, 1998; Fukuzawa *et al.*, 1999). In the latter, the *APC* gene, which is one of the key molecules in Wnt signaling, was found to be constitutively mutated (Kinzler and Vogelstein, 1996).

Increasing evidence suggests that Wnt signaling pathway also plays an important role in the genesis of sporadic hepatoblastomas. A high frequency (more than 60% in some reports) of somatic mutations in the *β-catenin* gene has recently been reported in sporadic tumors (Koch *et al.*, 1999; Wei *et al.*, 2000; Takayasu

*Correspondence: A Nakagawara, Division of Biochemistry, Chiba Cancer Center Research Institute, 666-2 Nitona, Chiba 260-8717, Japan; E-mail: akiranak@chiba-ccri.chuo.chiba.jp
Received 9 December 2003; revised 26 March 2004; accepted 1 April 2004; published online 28 June 2004

et al., 2001; Buendia, 2002). Mutant β-catenin proteins accumulate in the nucleus, resulting in stimulating transcription of the target genes such as *c-myc* and *cyclin D1* (Morin *et al.*, 1997; Polakis, 1999). Mutation in the *Axin* gene, whose product is an antagonist of nuclear accumulation of β-catenin, has also been found in HBL and may contribute to the pathogenesis of the tumors without *β-catenin* mutation (Taniguchi *et al.*, 2002; Miao *et al.*, 2003). However, the molecular mechanism underlying the pathogenesis of HBL is still largely unknown.

Recent progress in therapeutic strategies including intensive chemotherapy and liver transplantation improved the outcome of the patients with HBL. However, the prognosis of a significant fraction of the tumors still remains poor. The clinical markers currently used for HBL include staging, which is a major instrument for assessing prognosis (Hata, 1990), serum alpha-fetoprotein (AFP) (Mann *et al.*, 1978), mitotic activity (Haas *et al.*, 1989), DNA ploidy (Hata *et al.*, 1991), nuclear localization of β-catenin (Park *et al.*, 2001), p53 mutation (Oda *et al.*, 1995), and chromosomal alteration (Weber *et al.*, 2000). Serum AFP level is used as a diagnostic marker to monitor the tumor progression, responsiveness to the therapy, and recurrence after the treatment. Extremely high levels of serum AFP are reported to be associated with aggressiveness of the tumors with unfavorable outcome (van Tornout *et al.*, 1997), except some reports showing that there is no significant relationship between initial serum AFP levels and prognosis of the patients with HBL (Ortega *et al.*, 1991; von Schweinitz *et al.*, 1994). Moreover, the tumor with low levels of serum AFP often grows rapidly and is often reluctant to chemotherapy (von Schweinitz *et al.*, 1995). The other genetic markers including DNA ploidy, chromosomal aberration, and *p53* mutation are not so powerful clinical indicators. Even the nuclear localization of β-catenin and/or mutation of the *β-catenin* gene appear to lose their impact as a prognostic factor when combined with the grade of histological differentiation because of its close correlation with the latter (Takayasu *et al.*, 2001). Therefore, we may need to find novel markers to predict the patient's outcome in a comprehensive way.

To understand the molecular mechanism of the genesis and progression of HBL, as well as to develop a novel diagnostic and therapeutic system for the tumor, we have randomly cloned 10431 cDNAs expressed in primary HBL tissues and a normal infant's liver by using full-length-enriched oligo-capping cDNA libraries. In the present study, we have identified 86 genes differentially expressed between HBLs and their corresponding normal livers. One of such genes, *PLK1*, showed a significantly high expression in the formers as compared with the latters, and its high expression was significantly associated with poor prognosis of HBLs.

Results

Expression profiles of primary HBLs and a normal liver

To obtain the genes expressed in primary HBLs and normal infant's liver, we constructed oligo-capping cDNA libraries from two primary HBLs with increased AFP secretion (HMFT, HYST), a primary HBL without AFP secretion (HKMT), and a corresponding normal liver (HMFN). After cloning 3000 cDNAs from each of the four cDNA libraries, 2289, 2837, 2537, and 2768 clones from the libraries of HMFT, HYST, HKMT, and HMFN, respectively, were successfully end-sequenced. Homology search against the public databases of those 10431 clones by BLAST program revealed that 847 clones (8.1%) in total contained novel sequences which had not been annotated (Table 1).

To elucidate the gene expression pattern in each cDNA library, we compared expression profile of the known genes that appeared in three different kinds of libraries, a HBL with positive AFP (HMFT), a HBL with negative AFP (HKMT), and an infant's liver (HMFN) (Table 2). BodyMap (Okubo *et al.*, 1992) and a serial analysis of gene expression (SAGE) (Velculescu *et al.*, 2000) are very good methods to quickly provide quantification of the levels of all mRNAs in certain tissues and cell types by high throughput end-sequencing of cDNA clones. In this study, we applied the former method by counting cDNA clones to show each expression profile of HBL tumors or a non-tumorous tissue. Although each library consists of 3000 clones, which may be a rather small number, the frequency of each cDNA appearance provides a hint to understand each tissue's genetic background.

Overall, the most frequently appeared gene was *albumin* as expected, which was extremely low in the tumor with negative AFP. Genes involved in cellular structure and/or maintenance, glucose and lipid metabolisms, and a part of protein synthesis and its transport were frequently found in the normal liver library. On the

Table 1 Summary of the number of genes cloned from the cDNA libraries of hepatoblastomas and a normal infant liver of hepatoblastomas

Oligo-capping cDNA library	*No. of the clones*	*No. of the genes successfully end-sequenced*	*No. of the genes with unknown function*
Hepatoblastomas with positive AFP	6000	5126	323 (6.3%)
Hepatoblastoma with negative AFP	3000	2537	262 (10.3%)
Infant's liver	3000	2768	262 (9.5%)
Total	12000	10431	847 (8.1%)